Tectonophysics 478 (2009) 62–77

Contents lists available at ScienceDirect

Tectonophysics

journal homepage: www.elsevier.com/locate/tecto

Aeromagnetic exploration over the East Antarctic Ice Sheet: A new view of the Wilkes Subglacial Basin

Fausto Ferraccioli [a,*], Egidio Armadillo [b], Tom Jordan [a], Emanuele Bozzo [b], Hugh Corr [a]

[a] British Antarctic Survey, High Cross, Madingley Road, Cambridge, CB30ET, UK
[b] Dipartimento per lo studio del Territorio e delle sue Risorse, Univ. di Genova, Viale Benedetto XV,5, 16132 Genova, Italy

ARTICLE INFO

Article history:
Received 11 March 2008
Received in revised form 21 February 2009
Accepted 15 March 2009
Available online 24 March 2009

Keywords:
Aeromagnetic anomalies
East Antarctica
Wilkes Subglacial Basin
Backarc basin
Sedimentary basins

ABSTRACT

The Wilkes Subglacial Basin represents an approximately 1400 km-long and up to 600 km wide subglacial depression, buried beneath the over 3 km-thick East Antarctic Ice Sheet. Contrasting models, including rift models and flexural models, have been previously put forward to explain the tectonic origin of this enigmatic basin, which is located in the largely unexplored hinterland of the Transantarctic Mountains. A major aerogeophysical survey was flown during the 2005–06 austral summer to explore the Wilkes Subglacial Basin. Our new airborne radar dataset reveals that the Wilkes Subglacial Basin contains several subglacial basins, which are considerably deeper than previously mapped. Major aeromagnetic lineaments are detected from total field, pseudo-gravity, tilt derivative and Euler Deconvolution maps. These aeromagnetic lineaments reveal that the Wilkes Subglacial Basin and its sub-basins are structurally controlled. Comparison between aeromagnetic signatures over the Wilkes Subglacial Basin region and the Cordillera in North America, suggests that the basin contains a former broad backarc basin and fold-and-thrust belts, forming the transition between a Precambrian craton and the Ross Orogen. The eastern margin of the Wilkes Subglacial Basin is imposed upon the Prince Albert Fault System and the Priestley Fault. These faults may have been reactivated in the Cenozoic, as major strike–slip faults. The western margin of the Wilkes Subglacial Basin is located along the southern extension of the Precambrian-age Mertz Shear Zone and marks the edge of the Terre Adélie Craton. High-frequency aeromagnetic anomalies in the Wilkes Subglacial Basin image large volumes of Jurassic tholeiites, which were intruded into and extruded over Beacon sediments in a possible rift setting. Depth-estimates of magnetic anomaly sources and forward modelling indicate that major Cretaceous and Cenozoic rift basins with thick sedimentary infill, comparable to the deep Ross Sea Rift basins, are however unlikely beneath this part of the Wilkes Subglacial Basin. More localised graben-like features, with up to 1.5 km of sedimentary infill are identified in the Central Basins. These grabens may be transtensional features related to regional Cenozoic intraplate strike–slip deformation, which has been extensively mapped over the adjacent Transantarctic Mountains, and/or older Cretaceous grabens. Over 3 km deep sedimentary basins are also imaged beneath the Western Basins and are inferred to contain older sedimentary infill of Ross-age, based on recent dating of glacial erratics between Mertz and Ninnis Glacier.

1. Introduction

Aeromagnetic exploration over the West Antarctic Ice Sheet has provided an important geophysical tool to image tectonic structures, magmatic features and sedimentary basins associated with the underlying West Antarctic Rift System (Blankenship et al., 1993, 2001; Behrendt et al., 1996, 2004; Bell et al., 1998, 2006; Studinger et al., 2001). Systematic aeromagnetic surveying has also been performed over part of the Transantarctic Mountains (TAM) (e.g. Damaske, 1994; Ferraccioli and Bozzo, 1999), which form the uplifted flank of the West Antarctic Rift System (Stern and ten Brink, 1989; Stern et al., 2005; Bialas et al., 2007). In contrast, aeromagnetic exploration over the East Antarctic Ice Sheet (EAIS) in the hinterland region of the TAM is currently less extensive (Damaske et al., 2003; Studinger et al., 2004), due to its remoteness from logistic centres (Fig. 1).

The Wilkes Subglacial Basin (WSB) is the main topographic feature in this region, as detected from reconnaissance airborne radar data collected in the 70s (Drewry, 1976). It is a broad, almost 1400 km-long subglacial depression, buried beneath the over 3 km thick EAIS. In contrast to the over 2500 m high TAM, the mean bedrock elevation in the adjacent WSB is about 500 m below sea level (Drewry, 1983). The basin appears to narrow significantly southwards (Studinger et al., 2004), from its maximum width of almost 600 km (Steed, 1983) at the George V Coast (Fig. 1).

Early geophysical interpretations were derived from exploratory aeromagnetic lines and over-snow gravity traverses (Fig. 2a) and led to the suggestion that the WSB is a 400 km wide and approximately

* Corresponding author. Tel.: +44 1223 221577.
E-mail address: ffe@bas.ac.uk (F. Ferraccioli).

0040-1951/$ – see front matter © 2009 Elsevier B.V. All rights reserved.
doi:10.1016/j.tecto.2009.03.013

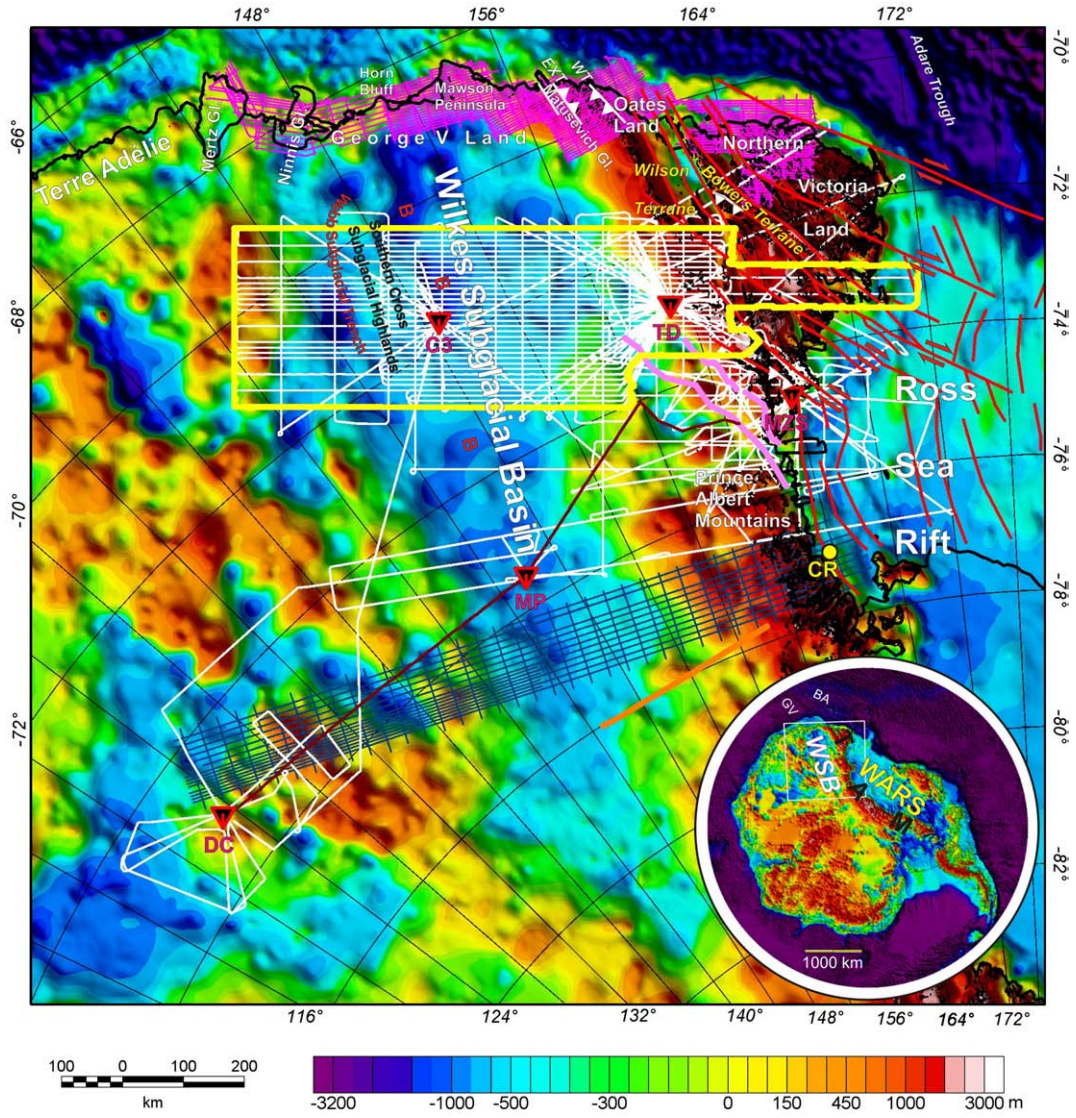

Fig. 1. Location of the new ISODYN/WISE aerogeophysical survey flown during the 2005–06 joint Italian–British campaign over East Antarctica (Ferraccioli et al., 2007), superimposed upon a bedrock topography map, derived from airborne radar data, and compiled within BEDMAP (Lythe et al., 2001). White lines show all our survey lines, while the yellow outline shows the area of the main aeromagnetic grid across the Wilkes Subglacial Basin, which we analyse as part of this study. Note the location of the bases and remote field camps used to accomplish the aerogeophysical survey, including Mario Zucchelli Station (MZS), Talos Dome (TD), Sitry (C3), Mid-Point (MP) and Dome C (DC). The location of recent aeromagnetic surveys across the Wilkes Subglacial Basin region is also shown. Magenta lines are the flight lines of the GITARA VI survey (Damaske et al., 2003; Ferraccioli et al., 2003), whilst blue lines are from the AEROTAM survey (Studinger et al., 2004). The orange line shows the East-93 traverse (ten Brink et al., 1997), while the brown line is the ITASE traverse (Ferraccioli et al., 2001). Note sub-basin B and the Webb Subglacial Trench (WST), which are separated by the Southern Cross Highlands (SCH), as mapped from Steed and Drewry (1982) and Drewry (1983). Also note the location of early Paleozoic thrust faults over Oates Land (EXT: Exiles Thrust; WT: Wilson Thrust) from Flöttmann and Kleinshmidt (1991). Red lines indicate the major Cenozoic strike–slip faults over Northern Victoria Land (Salvini et al., 1997). These strike–slip faults reactivated early Paleozoic thrust faults of the Ross Orogen (Federico et al., 2006), and may have induced Cenozoic transtensional rifting in the western Ross Sea Rift (e.g. Wilson, 1995). Pink lines depict the Prince Albert Fault System, which was imaged from previous aeromagnetic data as flanking the Prince Albert Mountains block of the Transantarctic Mountains (Ferraccioli and Bozzo, 2003). The location of the Cape Roberts (CR) drilling project, along the western margin of the Ross Sea Rift (Cape Roberts Science Team, 2000), is also shown. The inset shows our study area in Antarctica. Note the Wilkes Subglacial Basin (WSB), the Transantarctic Mountains (TAM) and the West Antarctic Rift System (WARS). GV and BA indicate the George V and Balleny transforms in the Southern Ocean that lie on strike with the Cenozoic strike–slip faults of Northern Victoria Land (Storti et al., 2007). Map projection: Lambert conical conformal with standard parallels 75°20′ S and −72°40′ S and central meridian 179° E. This projection has been utilised for all our maps.

3 km deep, fault-bounded, extensional sedimentary basin (Drewry, 1976; Steed, 1983). The existence of rift basins within the WSB was also inferred by Masolov et al. (1981) and Kadmina et al. (1983). However, more recent models, based upon sparse gravity and topography profiles, argued against the existence of a major extensional sedimentary basin in the WSB (Stern and ten Brink, 1989). These models favour instead a flexural origin for the WSB, induced by Cenozoic uplift of the TAM, coupled with the high rigidity of the East Antarctic Craton lithosphere (ten Brink and Stern, 1992). Gravity models based upon data from the East-93 traverse, which reached the eastern margin of the WSB (Fig. 2b) appear to be consistent with a flexural origin for the WSB, and do not require the presence of sedimentary infill in the basin (ten Brink et al., 1997). In contrast, gravity modelling along the recent ITASE traverse, which crossed the entire width of the basin, suggests possible crustal thinning beneath the WSB (Fig. 2c) and thin sedimentary infill (Ferraccioli et al., 2001).

We present new aeromagnetic and airborne radar data to study the controversial crustal structure and tectonic origin of the WSB, and to re-investigate the possible presence of sedimentary infill. Our interpretation is based on a set of enhanced aeromagnetic images, depth to magnetic source calculations, and 2D modelling. We also

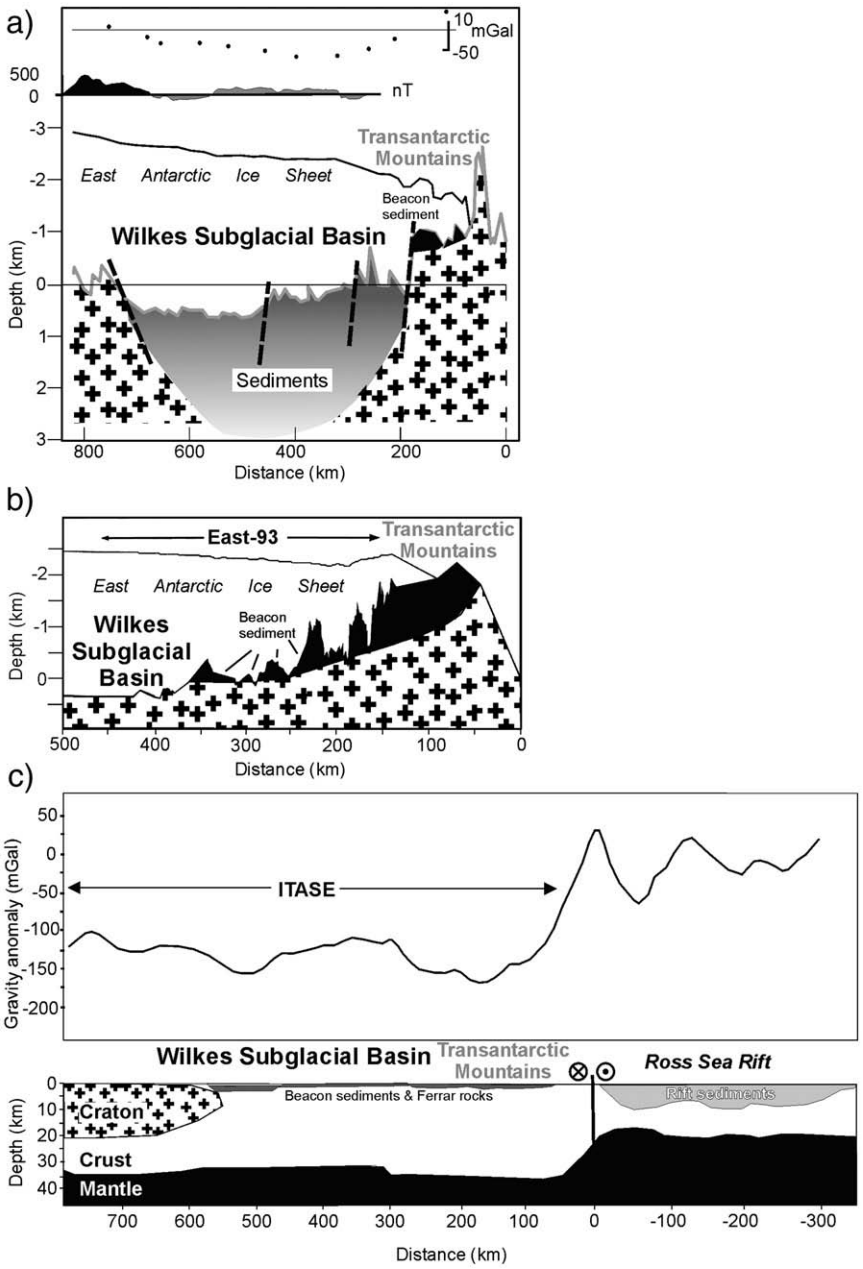

Fig. 2. Summary of contrasting tectonic models proposed for the Wilkes Subglacial Basin region. Early models (panel a) depicted the broad Wilkes Subglacial Basin as a major sedimentary basin, in light of its magnetic and gravity signatures along profiles crossing the basin (Drewry, 1976). Later models depicted the Wilkes Subglacial Basin as a glaciated flexural depression induced by Cenozoic uplift of the Transantarctic Mountains and containing no sedimentary infill (Stern and ten Brink, 1989; ten Brink and Stern 1992). Gravity signatures along the East-93 traverse (panel b) appear to support a flexural origin for the basin (ten Brink et al., 1997). Panel c shows a crustal model for the Wilkes Subglacial Basin, Transantarctic Mountains and adjacent Ross Sea Rift based upon ITASE and previous gravity data (modified from Ferraccioli et al., 2001). This crustal model has been interpreted as indicating that wide-mode crustal thinning may have occurred in the hinterland of the Transantarctic Mountains beneath the Wilkes Subglacial Basin (Ferraccioli et al., 2001).

exploit an analogy between aeromagnetic signatures over the WSB region and the northern Cordillera in Canada and Alaska to interpret the tectonic origin of this poorly known basin.

2. Geological and geophysical framework

2.1. Ross Orogen and East Antarctic Craton

Subduction and terrane accretion processes at the paleo-Pacific active margin of Gondwana formed the approximately 500 Ma old Ross Orogen (Ricci et al., 1997; Federico et al., 2006). Ross-age rocks are relatively well-exposed over northern Victoria Land. Subduction-related fore-arc and magmatic arc rocks have been interpreted from aeromagnetic (Finn et al., 1999; Ferraccioli et al., 2002, 2003) and geochemical data (Rocchi et al., 1998) over the Bowers Terrane and Wilson Terrane (Fig. 1), and remnants of oceanic crust under the Bowers Terrane have been inferred from deep electrical conductivity studies (Armadillo et al., 2004).

The location and nature of the boundary between the terranes affected by the Ross Orogen and the Precambrian East Antarctic Craton is subject to debate (Läufer et al., 2006). Long-wavelength aeromagnetic anomalies detected over the EAIS, just north of the Prince Albert Mountains (Fig. 1), were originally interpreted as reflecting unexposed Precambrian rocks of the East Antarctic Craton (Bosum et al., 1989). However, more recent aeromagnetic interpretations, coupled with magnetic susceptibility measurements in northern Victoria Land and Oates Land (Bozzo et al., 1992; Talarico et al., 2003, 2007), suggest that the sources of these aeromagnetic anomalies are Ross-age arc rocks,

assigned to the Granite Harbour Intrusives of the Wilson Terrane (Ferraccioli and Bozzo, 1999; Ferraccioli et al., 2003).

Precambrian rock units are exposed only much further west in Terre Adélie (Fig. 1) and provide a small window on Paleo-Proterozoic crust of the East Antarctic Craton (Oliver and Fanning, 1997). Granitoids in the area between Mertz and Ninnis Glaciers (Fig. 1), previously inferred to be 1850 Ma old (Oliver and Fanning, 1997), have been dated as 500 Ma, and are therefore interpreted as part of the Ross Orogen (Fanning et al., 2002).

2.2. Beacon Supergroup and Ferrar Group rocks

Erosion of the Ross Orogen formed the Silurian to Early Devonian Kukri Peneplain. The overlying Devonian to Jurassic Beacon Supergroup sediments were deposited in intracratonic (Woolfe and Barrett, 1995), foreland (Collinson, 1997), or intermontane basins (Isbell, 1999). Ferrar Group (Kirkpatrick Basalt and Ferrar Dolerite) tholeiitic rocks intrude and overlie Beacon Supergroup sediments and were emplaced at 184±1 Ma (Encarnacion et al., 1996). Present-day exposure of Ferrar rocks in the TAM suggests a narrow and elongate magmatic belt, the Jurassic Transantarctic rift (Schmidt and Rowley, 1986; Wilson, 1993), although no major rift-bounding faults have been identified so far (Elliot and Fleming, 2004). Aeromagnetic anomalies over George V Land have been used to trace Ferrar rocks also west of the TAM, from their exposures in the Mawson Peninsula and Horn Bluff areas (Fig. 1), along the northern margin of the WSB (Damaske et al., 2003). High-frequency magnetic anomalies detected along the ITASE traverse (Fig. 1) also suggest the occurrence of these rocks within part of the WSB (Ferraccioli et al., 2001).

2.3. Ross Sea Rift and the Transantarctic Mountains

The Ross Sea Rift basins are part of the West Antarctic Rift System (Fig. 1). These rift basins lie parallel to the TAM and to the WSB, and feature highly extended continental crust with thicknesses ranging from 16 to 24 km (Trey et al., 1999), and sedimentary infill up to 14 km thick (Cooper et al., 1987). Multiple stages of rifting have been inferred in the Ross Sea Rift, including broad-mode Cretaceous rifting, followed by narrow-mode Cenozoic rifting (Davey and Brancolini, 1995; Davey and De Santis, 2006; Huerta and Harry, 2007). The amount of Cenozoic extension in the Ross Sea Rift region is subject to significant debate. Some plate tectonic reconstructions (e.g. Lawver and Gahagan, 1994) and gravity modelling across the Ross Sea Rift (Karner et al., 2005) favour limited post-Cretaceous extension. However, marine geophysical evidence from the Adare Trough region suggests at least 180 km of Cenozoic extension (Cande et al., 2000). Cenozoic rifting within the western Ross Sea Rift may relate to right-lateral strike–slip faulting (Salvini et al., 1997; Storti et al., 2007) and/or to Adare Trough opening (Decesari et al., 2007).

Onshore and offshore structural patterns in the Cape Roberts area suggest the occurrence of transtensional rifting (Wilson, 1995; Hamilton et al., 2001; Ferraccioli and Bozzo, 2003). Drilling within the framework of the Cape Roberts Drilling Project (Fig. 1) indicates that the age of most of the sedimentary infill in the western Ross Sea Rift is late Eocene or younger (Cape Roberts Science Team, 2000). Apatite-fission track evidence suggests that the main phase of Cenozoic uplift of the TAM commenced at about 50 Ma, but was preceded in some regions by Cretaceous uplift (Fitzgerald, 2002). Geochronological data indicate that earliest occurrence of alkaline rift-related magmatism over Victoria Land is 48 Ma old (Tonarini et al., 1997; Rocchi et al., 2002).

Marine diatoms within the Sirius Group of the TAM could indicate marine sedimentation in the hinterland of the Transantarctic Mountains within the WSB during inferred periods of reduced extent of the EAIS in the Neogene (Webb et al., 1984). These marine diatoms could, however, be wind-blown rather than glacially transported by the EAIS, and might therefore not require the presence of any major Cenozoic marine basins in the WSB (Stroeven, 1997), consistent with the stabilist view of the EAIS (e.g. Sugden et al., 1995).

3. Aerogeophysical survey

An extensive aerogeophysical survey (Fig. 1) was flown over the EAIS during the 2005/06 Antarctic field-campaign as part of the collaborative UK–Italian ISODYN\WISE project. The survey covered part of the WSB and several tectonic blocks over the adjacent TAM (e.g. Van der Wateren and Cloetingh, 1999); it also extended to the western Ross Sea Rift and to Dome C region (Tabacco et al., 2006). Approximately 60,000 line km of new data were collected during 68 survey flights over an area of 767,300 km^2 (Ferraccioli et al., 2007). In our study we focus on the main aeromagnetic grid across the WSB, which was flown with a line spacing of 8.8 km, a tie line interval of 44 km, and a constant nominal elevation of 2400 m. In the western part of the survey grid, the line spacing was in part coarser (26.4 km) due to the impossibility of deploying extra fuel at the remote Sitry base camp (Fig. 1). The airborne survey platform was a British Antarctic Survey Twin Otter, equipped with airborne radar, aeromagnetic and airborne gravity sensors; a detailed description of the platform is reported in Ferraccioli et al. (2007).

4. New view of the bedrock topography in the Wilkes Subglacial Basin region

Knowledge of the regional subglacial topography in the WSB has so far derived from reconnaissance airborne radar data flown in the 70s by the SPRI/NSF/TUD programme (Drewry, 1976; Steed and Drewry, 1982; Steed, 1983; Drewry, 1983). Line spacing for these radar surveys was typically between 50 and 100 km and positioning relied on Inertial Navigation Systems and reckoning (Steed and Drewry, 1982). Early contour maps derived from these reconnaissance data suggested that the WSB represents a broad depression widening and deepening northwards, typically with depths of −500 to −750 m b.s.l. and reaching a maximum depth of 1670 m b.s.l. (Steed and Drewry, 1982). Two narrower sub-basins with depths below −1000 m were also recognised. One un-named basin (labelled B in Fig. 1) was imaged between Mawson Peninsula and Horn Bluff and was inferred to extend inland to approximately 74°S; the second basin was mapped between Horn Bluff and Ninnis Glacier and named by Drewry (1983) the Webb Subglacial Trench. A topographic high appeared to separate these basins (Fig. 1) and was named the Southern Cross Subglacial Highlands by Drewry (1983). While basin B is still recognisable from the more recent BEDMAP subglacial topography map for the entire Antarctic continent (Lythe et al., 2001) the linear Webb Subglacial Trench is less evident, likely due to smoothing associated with gridding (compare Drewry, 1983 and Fig. 1). The new bedrock topography map for the WSB and adjacent TAM shown in Fig. 3a was derived from our higher resolution and more accurately positioned airborne radar data over the region (Corr et al., 2007). The new map clearly confirms the existence of sub-basins in this part of the WSB. However, these sub-basins can now be recognised as being considerably deeper than previously thought and their trend and morphology is more accurately defined due to the tighter line spacing. These sub-basins have depths below −1500 m and up to 2100 m below sea-level. They are separated by mountain ranges and dissected, flat-lying, plateau-like features (named P and P′ in Fig. 3a). We name the newly mapped basins the Eastern, Central and Western Basins respectively. The area of the Western Basins includes the deep Webb Subglacial Trench of Drewry (1983).

5. New draped aeromagnetic anomaly map of the Wilkes Subglacial Basin region

Data processing required to obtain the total field aeromagnetic anomalies included base station correction, magnetic compensation,

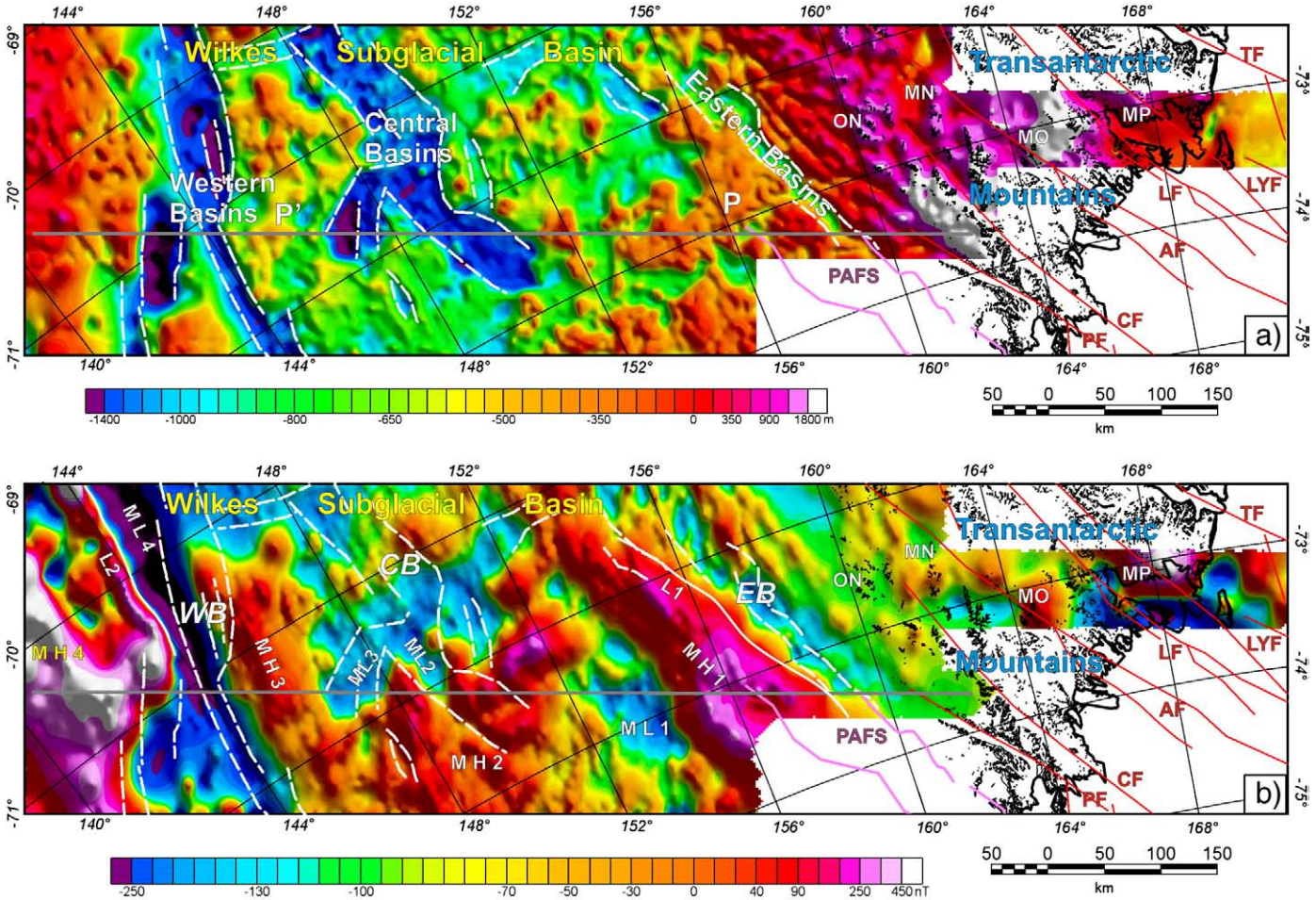

Fig. 3. a) New subglacial topography map for the Wilkes Subglacial Basin and adjacent Transantarctic Mountains derived from airborne radar data. Note the location of newly revealed sub-basins in the Wilkes Subglacial Basin region, including the Eastern, Central and Western Basins (dashed white line), which are flanked and separated by major subglacial highlands. Also note the location of flat-lying and incised plateau-like features P and P′. Grey line in this panel and following figures shows the location of the profile used for aeromagnetic interpretation, including depth to magnetic source calculations and 2D modelling. b) New aeromagnetic anomaly map for the Wilkes Subglacial Basin and adjacent Transantarctic Mountains. The location of the subglacial basins has been superimposed (EB: Eastern; CB: Central; WB: Western Basins respectively). Major aeromagnetic anomalies and lineaments have been labelled (see text for detailed description of the anomalies). The new aeromagnetic map reveals structural controls on the Wilkes Subglacial Basin. The position of major Cenozoic strike–slip faults over the adjacent Transantarctic Mountains (Salvini et al., 1997; Ferraccioli and Bozzo, 2003) is also reported in this and following figures (PAFS: Prince Albert Fault System; PF: Priestley; CF, AF, LF, LYF, TF: Campbell; Aviator; Lanterman; Leap Year; and Tucker faults respectively). ON: Outback Nunataks; MN: Monument Nunataks; MO: Mt. Overlord volcano; MP: Malta Plateau.

IGRF removal, levelling and microlevelling in frequency domain (Ferraccioli et al., 1998). This was followed by draping (Pilkington and Thurston, 2001) on our new bedrock topography map (Fig. 3a) to produce the aeromagnetic map shown in Fig. 3b. The drape interval was chosen to be equal to the mean distance to bedrock, i.e. 2800 m.

Over the TAM high-amplitude aeromagnetic anomalies (>500 nT) can be detected in the Malta Plateau (MP in Fig. 3b) region and delineate rift-related Meander Intrusives of Cenozoic age (Rocchi et al., 2002; Ferraccioli et al., this volume). A lower amplitude circular anomaly overlies Mt. Overlord volcano (MO). High-frequency anomalies in the Monument Nunataks region (MN) image Jurassic-age Ferrar Group rocks. NW–SE oriented magnetic anomalies west of the Outback Nunataks (ON) are interpreted as delineating the unexposed northern continuation of the Priestley Fault (Storti et al., 2001). The sources of the magnetic anomalies along the fault zone may represent sheared Granite Harbour Intrusives of Ross-age, or coeval mafic mylonites similar to those exposed in the Matusevich Glacier area (Fig. 1) along the Exiles Thrust (Flöttmann and Kleinshmidt, 1991; Ferraccioli et al., 2003; Talarico et al., 2003), to the north of our survey.

A remarkable NW–SE trending magnetic anomaly high (MH1) stretches for over 300 km along the eastern margin of the WSB and is flanked by a prominent magnetic lineament (L1). It is aligned with the Prince Albert Fault System detected from previous aeromagnetic imaging over the Prince Albert Mountains to the south of our grid (Ferraccioli and Bozzo, 2003). By analogy with previous aeromagnetic interpretations and models over the Prince Albert Mountains (Ferraccioli and Bozzo, 1999), we associate this long-wavelength anomaly with Ross-age magmatic arc intrusions. The new aeromagnetic data reveals that the Prince Albert Fault System and the Priestley Fault provide structural controls on the eastern margin of the WSB. In particular the Eastern Basins, which are located at the transition between the WSB and the TAM, are clearly aligned with the Prince Albert Fault System and its northern prosecution, which is imaged by magnetic lineament L1.

Within the WSB complex aeromagnetic patterns are observed. A broad magnetic low, punctuated by high-frequency magnetic anomalies, is observed between 156° E and 150° E (ML1 in Fig. 3b). In contrast, a broad magnetic high, with similar high-frequency magnetic anomalies superimposed upon it, dominates the aeromagnetic pattern between 150° E and 144° E (MH2). These high-frequency magnetic anomalies within the WSB overlie mesa topography detected from radar data (Fig. 3a), and are interpreted as delineating Beacon Supergroup rocks massively intruded by Ferrar tholeiites of Jurassic age, as is the case in the exposed Prince Albert Mountains further to the

south (Ferraccioli and Bozzo, 1999). Linear NNW–SSE to N–S oriented structural grain is observed within the WSB. Two broad magnetic lows are clearly imaged over the Central Basins (ML2, ML3). A broad magnetic high is detected over the highlands (P′ in Fig. 3a) separating the Western Basins from the Central Basins (MH3). A remarkable N–S oriented magnetic low overlies the Western Basins (ML4). The axis of the magnetic low roughly corresponds to the western flank of the north-westernmost basin (Webb Subglacial Trench of Drewry, 1983). The aeromagnetic pattern changes remarkably along the western flank of the WSB. Much higher amplitude aeromagnetic anomalies (up

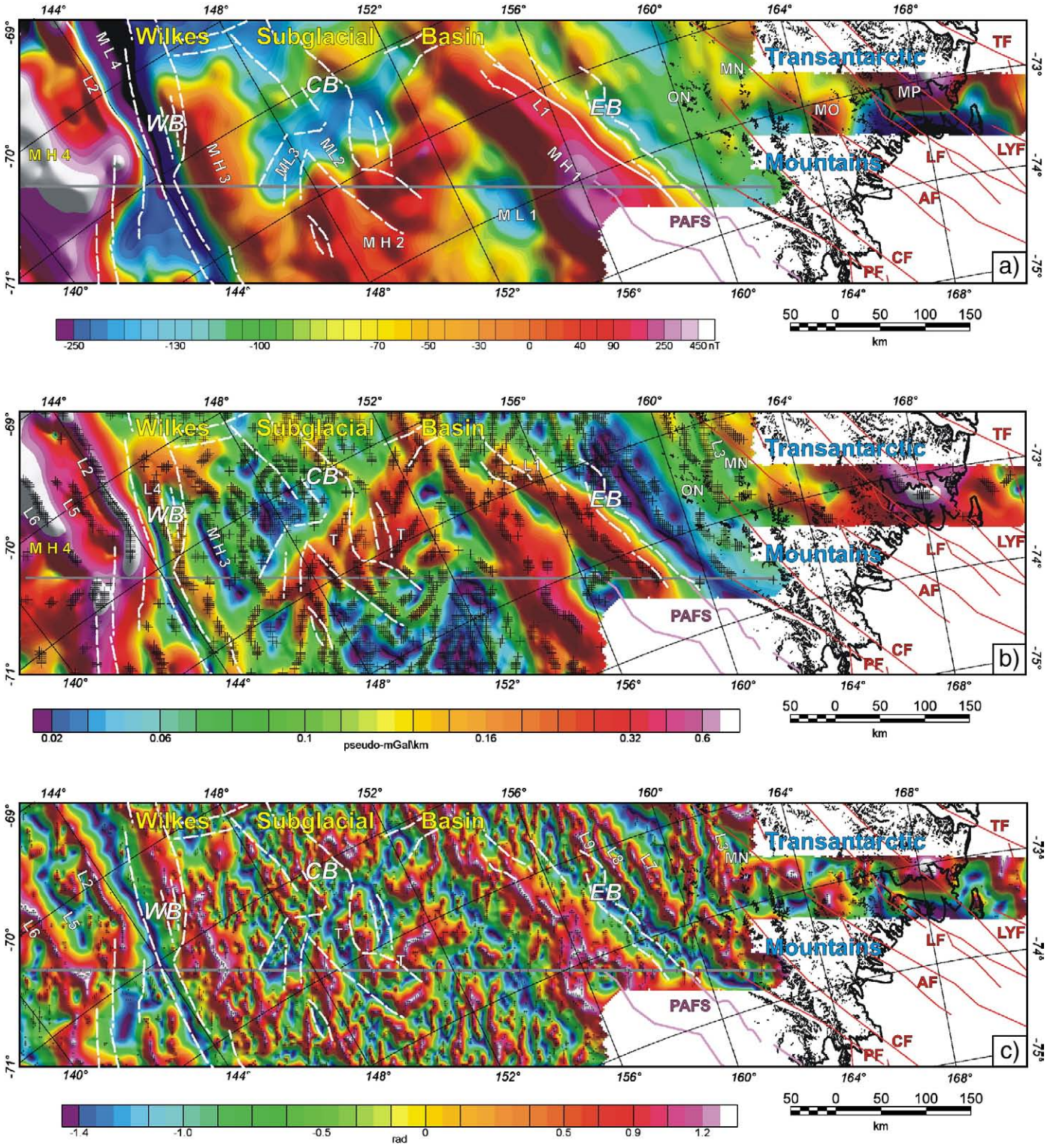

Fig. 4. Enhanced aeromagnetic images over the Wilkes Subglacial Basin and adjacent Transantarctic Mountains. Panel a shows the aeromagnetic anomalies upward continued to a 10 km level to enhance signatures from deeper basement sources. Panel b is the maximum horizontal gradient of pseudo-gravity, which can be used to detect the edges of magnetic source bodies and magnetic lineaments. The structural grain in the Wilkes Subglacial Basin region is apparent. Panel c is a tilt derivative map, which is effective in emphasising shallow-source anomalies and structural features. Note for example a set of NNW–SSE trending lineaments along the eastern flank of the Eastern Basin, interpreted as representing possible splays of the Priestley Fault, and other lineaments in the area of the Central and Western Basins and their flanks, likely imaging major sub-ice fault systems.

to 900 nT) are detected over the highlands flanking the WSB (MH4). A N–S oriented, high-frequency magnetic anomaly (L2), is interpreted as delineating a major fault along the western margin of the WSB.

6. Enhanced aeromagnetic anomaly maps

A set of enhanced aeromagnetic images were compiled for advanced anomaly interpretation over the WSB and adjacent TAM. Fig. 4a displays an upward continued aeromagnetic anomaly map at a 10 km observation level, which enhances signatures arising from deeper geological sources at the expense of shallower ones (Blakely, 1995). This map is effective in smoothing out the magnetic patterns of the shallow-level Ferrar rocks of Jurassic age and enhances the signatures arising from deeper seated magmatic arc rocks of the Ross Orogen. High-frequency magnetic anomalies aligned with the Priestley Fault have now disappeared, as have the high-frequency anomalies superimposed upon magnetic low ML1 and magnetic high MH2 in the WSB, which we attributed to Ferrar Group rocks. The long-wavelength magnetic highs over the eastern and western flanks of the WSB (MH1–MH4) are enhanced, suggesting deeply rooted source bodies.

To detect the edges of magnetic source-bodies and lineaments we utilised the peaks of the maximum horizontal gradient of pseudo-gravity (Cordell and Grauch, 1985; Blakely and Simpson, 1986). The map (Fig. 4b) enhances the NW–SE to NNW–SSE structures at the transition between the TAM and the WSB that represent the continuation of the Priestley Fault (Storti et al., 2001) and the Prince Albert Fault System (Ferraccioli and Bozzo, 2003). A subtle N–S oriented lineament can also be detected west of the Monument Nunataks (L3) and is interpreted as a fault splay connecting the Campbell Fault and the Aviator Fault. Within the WSB, the map enhances the NNW–SSE oriented structural grain and images several transverse NE–SW magnetic trends, in particular along the flanks of the Central Basins (T). A prominent magnetic lineament (L4) can be recognised along the axis of the northernmost Western Basins (in the Webb Subglacial Trench of Drewry, 1983), and marks the western flank of magnetic high MH3. Two other N–S oriented magnetic lineaments, in addition to the previously traced lineament L2, can be recognised within the magnetic high MH4, along the western flank of the WSB (L5, L6).

To further enhance imaging of shallow sources we utilised a modified tilt derivative filter (Cooper and Cowan, 2006), which is shown in Fig. 4c. The map reveals at least three NNW–SSE trending lineaments with an apparent en echelon arrangement (L7–L9), which we interpret as representing fault splays associated to the Priestley Fault. These lineaments appear to truncate N–S structural grain flanking the Monument Nunataks region. NNW–SSE, N–S and NE–SW structural grain within the WSB is evident from the tilt derivative map.

7. Depth estimates

7.1. 3D Euler Deconvolution

To estimate depth and location of magnetic sources we applied 3D Euler Deconvolution, which involves first calculating the horizontal and vertical derivatives of the total field magnetic data (Reid et al., 1990). This is followed by the application of Euler's homogeneity equation, with the degree of homogeneity expressed as a "structural index" (SI).

Fig. 5 shows the results for SI = 0 and for a window size 5 × 5 grid cells (11,000 m). This structural index is typically utilised to image contacts and regional faults with a large throw. Over the TAM N–S oriented magnetic lineaments can be detected between the Campbell Fault and the Aviator Fault in the Monument Nunataks area (e.g. L3). Shallow magnetic lineaments can be identified along the inferred continuation of the Priestley Fault (L7) west of the Outback Nunataks. The Euler Deconvolution map clearly confirms structural controls on both flanks of the WSB. Magnetic lineament L1, lying on strike with the Prince Albert Fault System, is clearly identified. A prominent magnetic lineament is identified along the axis of the north Western Basins (L4) and flanks magnetic high MH3. Along the western flank of the WSB magnetic lineament L2 appears to be formed by two segments: the northern part is N–S trending, while the southern part is NNE–SSW oriented. Overall a sinuous tectonic boundary appears to flank magnetic high MH4.

Within the WSB shallow solutions are found, typically in the range between 1 and 3.5 km below sea level. Given that subglacial topography in the Central Basins region reaches depths of 1.5 km below sea level, a maximum of 2 km of sedimentary infill is estimated. The depth estimates beneath the Western Basins are generally deeper (4–7 km) and the subglacial topography reaches depths of 2 km below sea level. Hence a thicker sedimentary infill (>3 km) is possible beneath the Western Basins. The map also confirms the existence of N–S and NNE–SSW to NE–SW trends within the WSB, in particular in the Central Basins area. A NW–SE oriented trend is detected further to the east at 156° E (L10) which forms the eastern flank of magnetic low ML1.

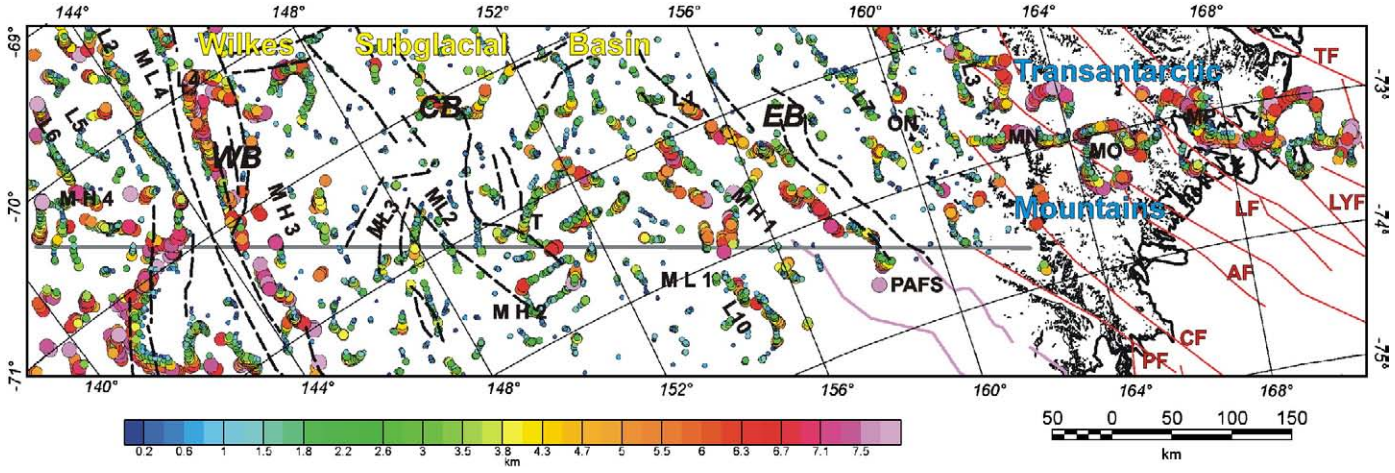

Fig. 5. Three-dimensional Euler Deconvolution over the Wilkes Subglacial Basin and adjacent Transantarctic Mountains for structural index SI = 0. Shallow-source solutions over the Wilkes Subglacial Basin region are keys to estimating the possible thickness of sedimentary infill in the basin. Note the contrast between generally shallower solutions in the Central Basins area and the deeper solutions over the Western Basins. The map is also useful to determine the location of structural features and their depth. For example, note the linear cluster of shallow-source solutions along the western flank of the Wilkes Subglacial Basin (magnetic lineament L2), and the deeper linear cluster along its eastern flank (lineament L1), interpreted as representing the buried continuation of the Prince Albert Fault System.

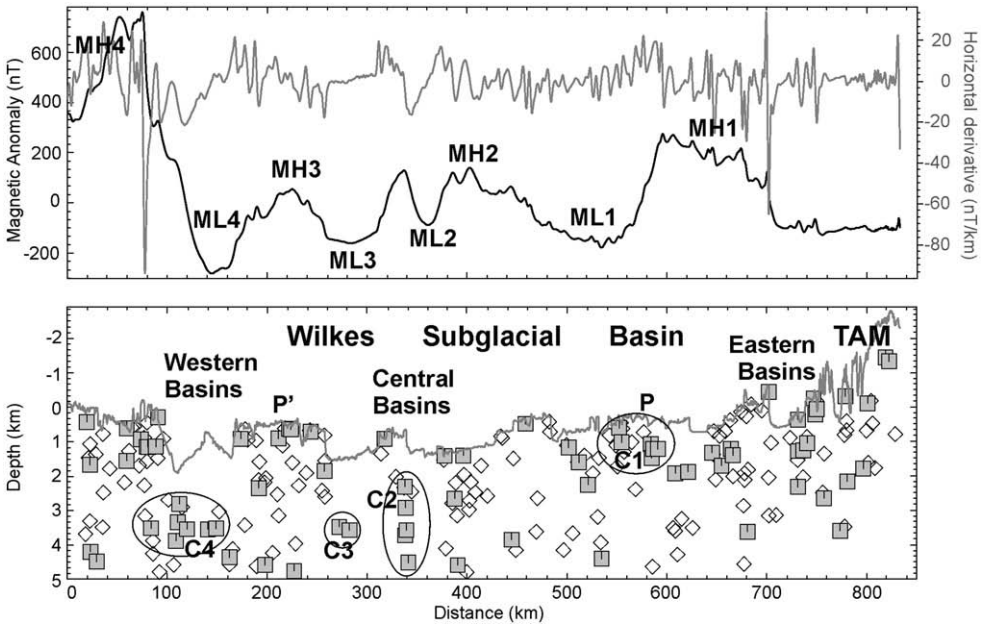

Fig. 6. Two-dimensional Werner Deconvolution along a profile (grey line in Figs. 3–5) used to estimate the depth to magnetic sources across the Wilkes Subglacial Basin. The black line in the upper panel shows the total field aeromagnetic anomaly data along the profile, while the grey line is the calculated horizontal derivative of the magnetic anomaly field. Note the lack of high-frequency magnetic anomalies over magnetic lows ML2, ML3 and ML4, suggesting the lack of shallow-sources beneath these regions (i.e. part of the Central Basins, and the Western Basins). Grey squares represent clusters of contact solutions, while diamonds are dyke-like solutions. Shallow solutions are identified over the plateau regions P and P′ suggesting that any possible sedimentary infill over these regions is thin. However, deeper clusters of solutions are identified beneath the Central and Western Basins, suggesting the possible occurrence of thicker sedimentary infill beneath these basins.

7.2. 2D Werner deconvolution

We used two-dimensional Werner deconvolution (Ku and Sharp, 1983) to estimate the depth to magnetic sources along a sample profile across the WSB (Fig. 6). A deconvolution window of several data points is shifted along the profile and, at each position, simultaneous magnetic field equations are solved by a nonlinear Marquardt least squares method. After several iterations, we selected a deconvolution window size range from 6 to 36 km, which proved to be suitable for the wavelengths of the main magnetic anomalies along the profile. The method provides depth estimates and horizontal location for contact and dyke-like sources.

Shallow solutions correspond to high-frequency magnetic anomalies detected over the TAM east of the Eastern Basins, which image outcrops of Jurassic Ferrar rocks (GANOVEX Team, 1987). A similar cluster of shallow solutions (C1) is detected beneath high-frequency magnetic anomalies along the western margin of an approximately 80 km wide plateau-like feature (P) located in the WSB. We interpret these anomalies as revealing Jurassic Ferrar rocks intruding Beacon Supergroup sediments. Our estimates yielded depths of about 1 km below sea level (500 m below the bedrock surface) for the sources of these anomalies, suggesting a maximum of 500 m of post-Jurassic sediments in this part of the WSB. Thicker (>1.5 km) sedimentary infill is however possible beneath prominent magnetic lows (ML2, ML3) over parts of the Central Basins, where deeper and relatively poorly clustered solutions were identified (C2, C3). Thick sedimentary infill (>2 km) is also possible beneath the Western Basins, where cluster C4 lies at a mean depth of about 3.5 km. The presence of thick sedimentary infill in the area of the Western Basins is consistent with the depth estimates derived from 3D Euler Deconvolution over this region (Fig. 5).

8. Magnetic modelling across the Wilkes Subglacial Basin

A simple two-dimensional forward magnetic model was calculated in GM-SYS® to provide some constraints on the possible geometries of the magnetic source bodies at depth in the WSB region (Fig. 7). The results of 2D Werner Deconvolution were superimposed as a guide for the starting model. Three layers were considered in this starting model: 1) a non-magnetic sedimentary layer ($0 \cdot 10^{-3}$ SI); 2) a variably magnetised upper crustal layer ($10–22 \cdot 10^{-3}$ SI), assigned to the Beacon Supergroup, massively intruded by magnetic Ferrar rocks (comparable to previous magnetic models for the Prince Albert Mountains—e.g. Ferraccioli and Bozzo, 1999); 3) a magnetised basement layer ($5 \cdot 10^{-3}$ SI).

The long-wavelength magnetic highs MH1, MH2 and MH3 are modelled by several-km thick intrusions. The thickness of the intrusion causing the long-wavelength magnetic high MH1 is approximately 10 km, if one assumes an apparent susceptibility of $65 \cdot 10^{-3}$ SI, and a maximum width of about 200 km at the base of the intrusion. Comparable magnetic susceptibilities and thicknesses of source bodies have been observed over the deep roots of several magmatic arc batholiths, e.g. over California, Japan and Antarctic Peninsula (Finn, 1994; Johnson, 1999). However, measured magnetic susceptibilities over exposed Ross-age arc rocks over Oates Land are generally lower ($<30 \cdot 10^{-3}$ SI) (Ferraccioli et al., 2003), implying that the thickness of the magmatic arc may be even greater than we modelled. Two relatively smaller and relatively less thick intrusions, with lower apparent susceptibilities, are introduced in the model to explain magnetic highs MH2 and MH3. An additional intrusion was introduced between magnetic lows ML2 and ML3 in the area of the Central Basins. These intrusions, with a maximum extent of approximately 100 km, are comparable in size and magnetisation to back-arc batholiths extensively mapped over the Antarctic Peninsula magmatic arc (Johnson, 1999).

The much higher amplitude magnetic high MH4 is modelled as arising from an over 14 km thick body with an apparent susceptibility of $110 \cdot 10^{-3}$ SI, which we interpret as the leading edge of mafic rocks assigned to the Precambrian East Antarctic Craton. Notably high magnetic susceptibilities ($>30 \cdot 10^{-3}$ SI) have been measured over outcrops of Precambrian rock assemblages west of Mertz Glacier (Talarico et al., 2001), in Terre Adélie (Fig. 1).

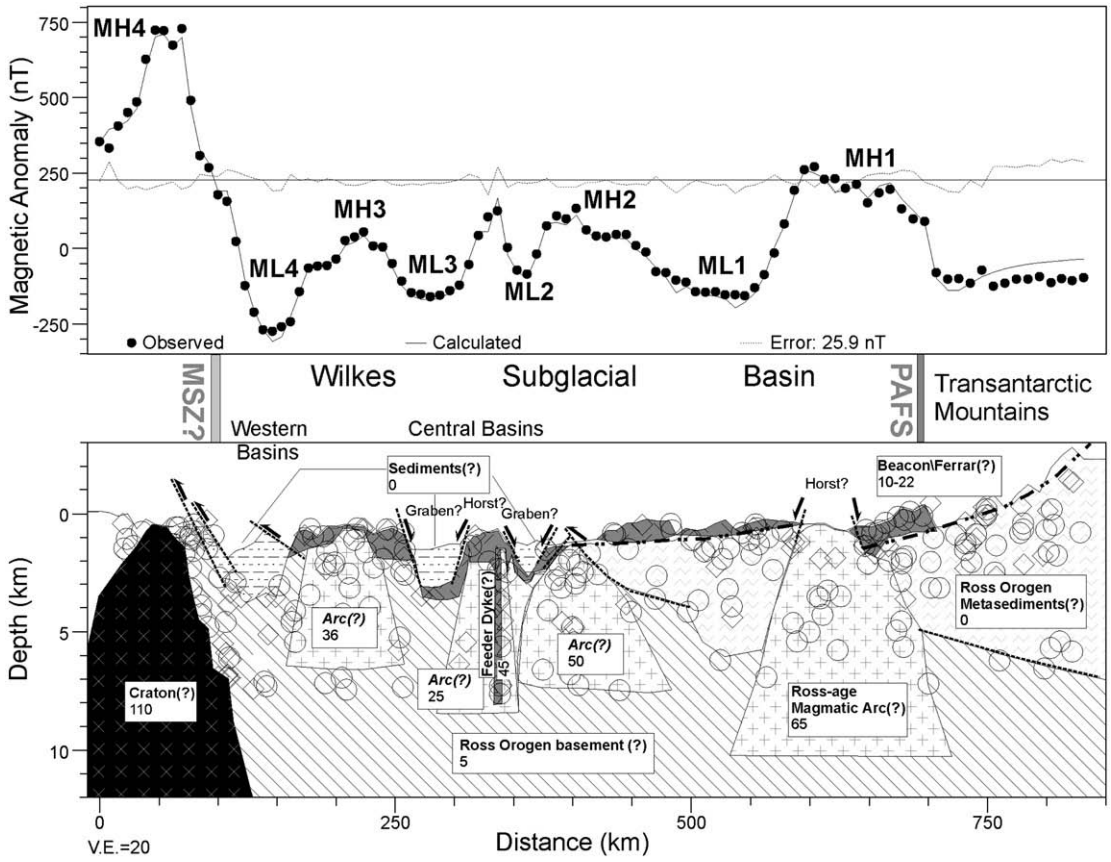

Fig. 7. Two-dimensional interpretative magnetic model across the Wilkes Subglacial Basin. The upper panel shows the observed and calculated anomalies and the model error. The lower panel is our preferred crustal model and interpretation, superimposed upon depth estimates derived from Werner Deconvolution, which were used to construct our starting model (circles and diamonds represent contact and dyke-like solutions respectively). Apparent magnetic susceptibilities for model bodies are in 10^{-3} SI. Long-wavelength magnetic highs in the Wilkes Subglacial Basin are accounted for by thick magnetic intrusions. These magnetic bodies are interpreted to represent arc intrusions of Ross-age, intruding non-magnetic metasediments and magnetic basement also inferred to have been affected by the Ross Orogen. In contrast, the higher amplitude magnetic high observed along the western flank of the Wilkes Subglacial Basin is interpreted as the leading edge of the Precambrian Craton. High-frequency anomalies across the Wilkes Subglacial Basin region are modelled as sheet-like bodies, interpreted as Beacon Supergroup sediments, extensively intruded by Jurassic tholeiites of the Ferrar Group, or possible feeder dykes. Magnetic lows over the Central and Western Basins are explained by sedimentary basins. Note graben-like features beneath part of the Central Basins, which may contain post-Jurassic sediment. Dash–dot line shows possible flexural profile of the subglacial topography and Kukri Peneplain, which likely relates to Cenozoic uplift processes of the TAM (e.g. ten Brink et al., 1997). However, our aeromagnetic interpretation predicts that the Wilkes Subglacial Basin is a structurally controlled basin, rather than a simple flexural downwarp. Its flanks are imposed upon major faults such as Mertz Shear zone (MSZ) and Prince Albert Fault System (PAFS) (see text for further explanation).

Magnetic lows ML2, ML3, ML4 over the Central and Western Basins are modelled by introducing sedimentary basins with thicknesses ranging from 1 to 3 km, in general agreement with depth estimates derived from Werner Deconvolution. Longer wavelength magnetic lows on both sides of MH1 are attributed to non-magnetic metasediments of the Ross Orogen, consistent with measured susceptibilities over outcrops of these rocks in the adjacent TAM (Bozzo et al., 1995). The remarkable magnetic lineaments imaged on the flanks of the WSB, are modelled as major crustal faults, representing the prosecution of the Prince Albert Fault System and Mertz Shear Zone respectively, as addressed further in the discussion.

9. Discussion

9.1. Subglacial geology in the Wilkes Subglacial Basin

A new geological sketch map for the WSB (Fig. 8) was compiled based upon the analysis of total field and enhanced aeromagnetic maps and the results of magnetic modelling. The map shows the location of Cenozoic Meander Intrusives (MI), McMurdo Volcanics (CV) and Jurassic Ferrar Group rocks (black F in Fig. 8) over the TAM. High-amplitude aeromagnetic anomalies typically associated with Cenozoic rift-related magmatic rocks of the TAM rift flank and the Ross Sea Rift (Behrendt et al., 1996; Ferraccioli and Bozzo, 1999) are notably lacking over this part of the WSB, indicating that any possible Cenozoic crustal extension within the WSB basin was largely amagmatic. However, Jurassic Ferrar Group rocks (white F in Fig. 8) are interpreted to extend from the TAM across the WSB region, as far west as 144° E. Our map also images the distribution of Ross-age arc rocks, which we interpret to extend over a broad, approximately 400 km wide area beneath the WSB. West of the WSB, highly magnetic Precambrian rocks, assigned to the East Antarctic Craton are inferred. Finally, sedimentary basins (S) have been identified as underlying the Central and Western Basins.

Major tectonic structures are also identified. Over the TAM we map the inferred continuation of NW–SE oriented Cenozoic fault belts, such as the Aviator Fault, the Campbell Fault and the Priestley Fault (Salvini et al., 1997; Storti et al., 2001) and associated NNW–SSE to N–S trending fault splays. A remarkable NW–SE oriented tectonic boundary is delineated along the eastern margin of the WSB, and is interpreted as the prosecution of the Prince Albert Fault System (Ferraccioli and Bozzo, 2003). Major faults are also inferred to flank sedimentary basins identified in the Central Basins area. The NW–SE oriented faults in the Central Basins area, lie parallel to the major fault belts of the TAM. NNW–SSE and N–S faults are also inferred, and may represent secondary fault splays of the master faults, as is the case in the TAM (Salvini et al., 1997). NE–SW oriented lineaments are also identified over the Central Basins region and may represent major transverse

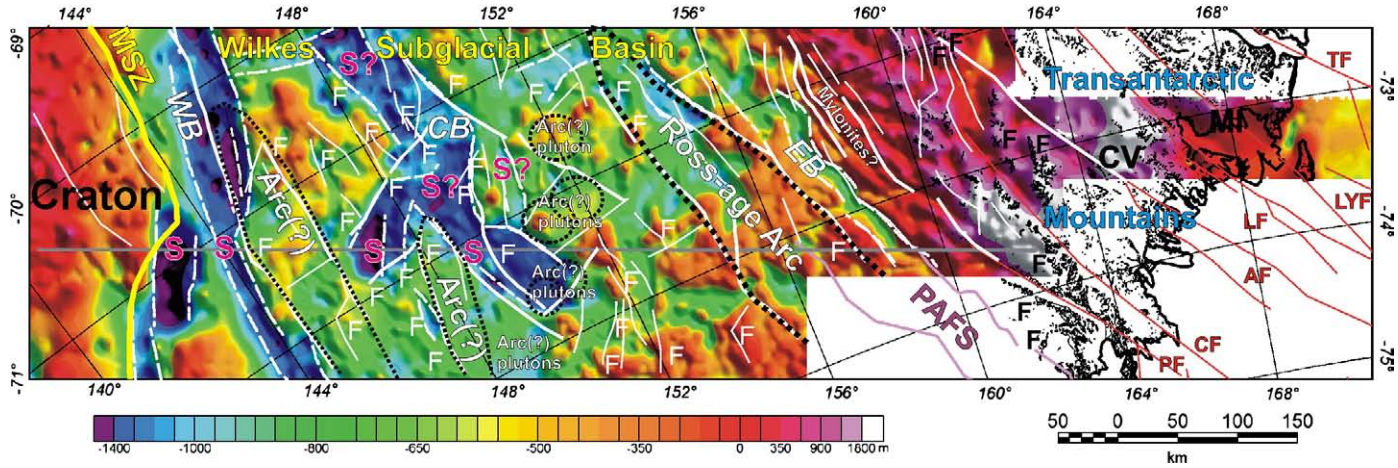

Fig. 8. New geological sketch map over the study area derived from the interpretation of aeromagnetic images, depth to source estimates, and magnetic modelling, superimposed upon bedrock topography. The map shows the location of major aeromagnetic lineaments (white lines) interpreted as delineating faults over the Transantarctic Mountains and Wilkes Subglacial Basin region. Over the Transantarctic Mountains magnetic lineaments trace subglacial fault belts representing the continuation of the Priestley (PF), Campbell (CF) and Aviator (AF) faults. The Priestley Fault and Prince Albert Fault System (PAFS) provide structural controls on the location of the Eastern Basin and the eastern margin of the Wilkes Subglacial Basin. Structurally controlled sedimentary basins (S) are also identified in the area of the Central Basins (CB). The Western Basins are also interpreted to be structurally controlled and include sediments, interpreted to be thrust towards the Precambrian craton (see magnetic model in Fig. 7). The location of the inferred Ross-age arc rocks is also shown (black stipple), as are the Jurassic Ferrar Group rocks (F).

faults. A major fault is inferred to run along the axis of the broad northern Western Basins. South of 70° S the fault zone appears to be located along the eastern flank of a narrower, linear, subglacial basin.

9.2. Tectonic origin of the Wilkes Subglacial Basin

To place our new aeromagnetic results in a broader regional context we first compiled a new subglacial topography map for the WSB and adjacent TAM region (Fig. 9). The new regional subglacial topography map was obtained by combining existing ice thickness data from reconnaissance (Drewry, 1983) and more detailed surveys (Studinger et al., 2004) with our new ISODYN-WISE radar data over the WSB. A more description of data integration and gridding procedures and differences with the previous BEDMAP compilation (Lythe et al., 2001) is described elsewhere.

The subglacial geology as derived from our aeromagnetic interpretation is superimposed on this map. The WSB can now clearly be recognised as being a structurally controlled basin. This is at odds with a purely flexural origin for the WSB induced by Cenozoic uplift of the TAM, proposed from previous gravity modelling (Stern and ten Brink, 1989; ten Brink and Stern 1992, 1997). The role of inherited tectonic structures must, in our view, be addressed to explain both the tectonic origin and later evolution of the WSB. The eastern flank of the WSB is controlled by a major Ross-age fault belt. Faults are inferred from aeromagnetic evidence to extend from the Matusevich Glacier area (Damaske et al., 2003; Ferraccioli et al., 2003), where the Ross-age Exiles Thrust outcrops (Flöttmann and Kleinshmidt, 1991), to the Priestley Glacier region, where the Boomerang Thrust lies (Skinner, 1991). K–Ar age data and structural evidence suggest that a late Ross-age pop-up structure exists in the Wilson Terrane (Flöttmann et al., 1993). The pop-up is formed by bivergent thrusts including the Wilson Thrust, the Exiles Thrust and the Boomerang Thrust, and extends from Oates Land to the Ross Sea Coast (Adams, 2006). Further to the west, long-wavelength aeromagnetic anomalies image Ross-age arc rocks emplaced along the prosecution of the Prince Albert Fault System. Similar aeromagnetic anomalies have been previously detected over the Mawson Peninsula region (Damaske et al., 2003) and may be imaging the northern extension of the Ross-age magmatic arc along the eastern margin of the WSB.

The western margin of the WSB is also structurally controlled. A major right-lateral strike–slip fault has been mapped from geological data in the Mertz Glacier region and named the Mertz Shear Zone (Talarico and Kleinschmidt, 2003). It is interpreted to mark the tectonic boundary between the Precambrian East Antarctic Craton, which outcrops in Terre Adélie, and 500 Ma old granitoids of the Ross Orogen, outcropping between Mertz and Ninnis Glacier (Talarico and Kleinschmidt, 2003). ^{40}Ar–^{39}Ar data from mylonitic rocks indicate ductile deformation under greenschist-facies conditions at 1502 ± 9 Ma along the Mertz Shear Zone and reveal no evidence for Ross-age reactivation (Di Vincenzo et al., 2007). We interpret the major aeromagnetic lineament imaged along the western flank of the WSB as the buried southern continuation of the Mertz Shear Zone. Our aeromagnetic interpretation for the occurrence of the tectonic boundary between the Precambrian Craton and the Ross Orogen along the western margin of the WSB is also supported by independent satellite magnetic anomaly data (Maus et al., 2002). A high-amplitude positive satellite magnetic anomaly over Terre Adélie reflects Paleo and Mesoproterozoic mafic igneous crust, similar to the crust of the Gawler Craton in Australia, in contrast with the prominent satellite magnetic low over George V Land, interpreted as reflecting Neoproterozoic to Cambrian sedimentary basement rocks affected by the Ross Orogen (Finn et al., 2006).

To gain further insight into the tectonic origin of the WSB we propose an analogy with the better known northern Cordilleran fold-and-thrust belt in Canada and Alaska, which forms the northwestern margin of the North American Craton (Reed et al., 2005). The regional magnetic anomaly patterns we observed over the WSB region mimic those imaged over the northwest Cordilleran active margin of the North American Craton (Saltus and Hudson, 2007), as shown in Fig. 10. In both cases long-wavelength magnetic highs mark magmatic arc terranes linked to subduction of oceanic lithosphere and a broad magnetic low delineates a wide backarc mobile belt. Long-wavelength and high-amplitude magnetic anomalies correlate with mafic crust at the edge of the stable craton, which forms a buttress for the fold-and-thrust belt.

Our tectonic model predicting that the WSB includes a fold-and-thrust belt located between the East Antarctic Craton and the Ross Orogen, is consistent with geological evidence over Oates Land (Läufer et al., 2006) and over the coeval Delamerian Orogen in Australia (Flöttmann et al., 1993, 1994). It is also supported by aerogravity signatures over the western margin of the WSB further south, which have been interpreted as indicating the presence of a major fold-and-thrust belt at the margin of the East Antarctic Craton (Studinger et al., 2004). The significant width of the transition zone we imaged between the Ross-age magmatic arc and the Precambrian craton could be

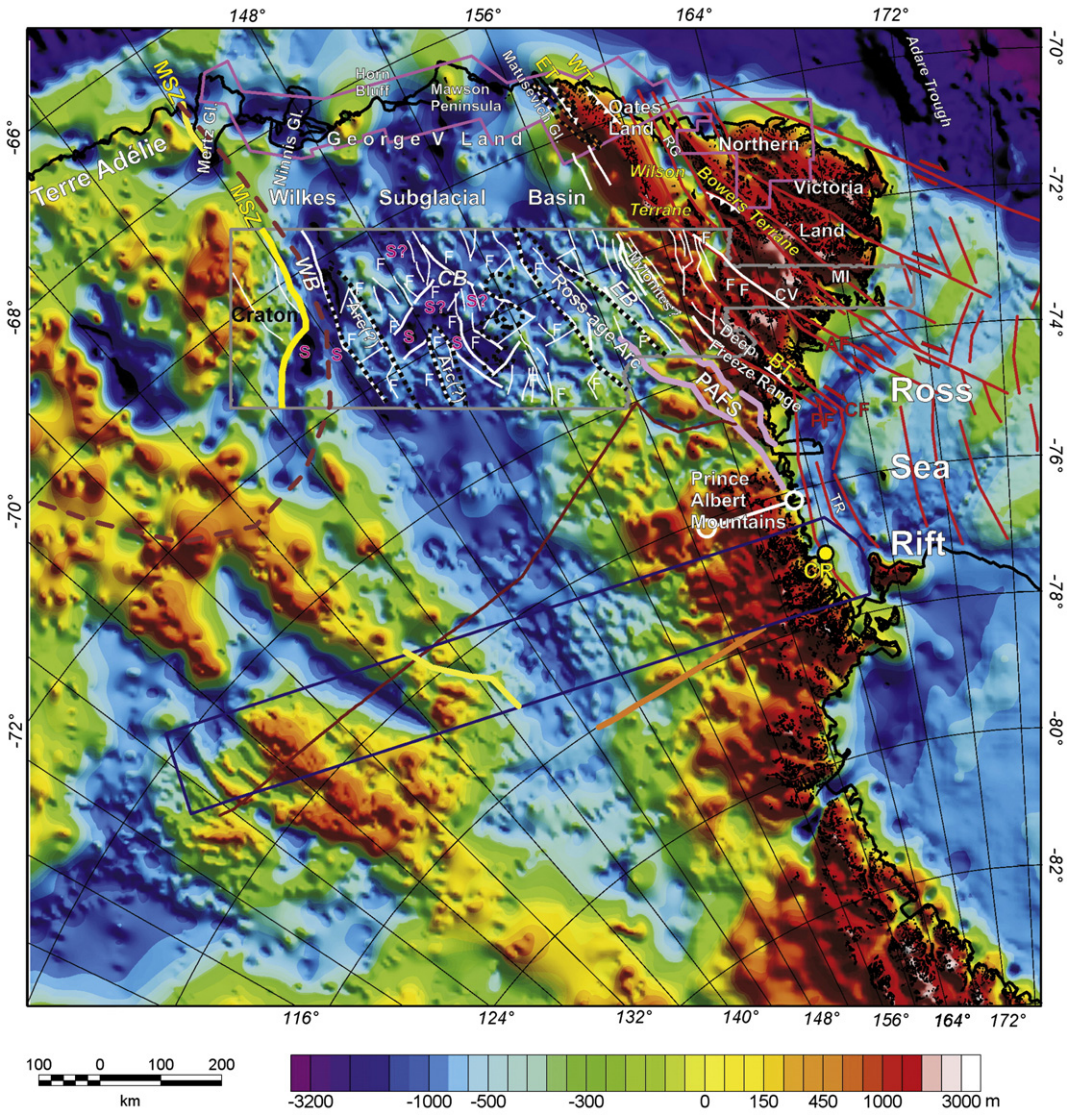

Fig. 9. Aeromagnetic interpretation (Fig. 8) displayed over a new bedrock topography map, obtained by combining our (Fig. 3c) and previous airborne radar data complied within BEDMAP (Fig. 1). The Precambrian-age Mertz Shear Zone (MSZ), flanking the Terre Adélie Craton and forming the western boundary of the Ross Orogen (Di Vincenzo et al., 2007), is shown as a yellow line in the Mertz Glacier area. Further to the south, in our survey grid area (grey outline) the yellow line denotes the prominent aeromagnetic lineament along the western flank of the Wilkes Subglacial Basin, which we interpret as imaging the subglacial extent of the Mertz Shear Zone. Major sedimentary basins in the area of the Western Basins appear to be located along the tectonic boundary between the craton and the Ross Orogen. The dashed brown line indicates the edge of the high-amplitude satellite anomaly, interpreted as delineating the extent of the Precambrian craton, unaffected by the Ross Orogen (Finn et al., 2006). The yellow line in the area of the AEROTAM sssaerogeophysical survey (blue outline) is the interpreted boundary of the Precambrian craton further south (Studinger et al., 2004; Finn et al., 2006). Brown line shows the ITASE traverse, while the white line with circles shows the location of the ACRUP seismic experiment, where crustal thickness estimates have been derived for the Transantarctic Mountains (Della Vedova et al., 1997). Orange and black outline indicates the area of the previously detected Matusevich aeromagnetic anomaly, associated with arc rocks and scraps of ultramafic rocks of Ross-age (Ferraccioli et al., 2003), emplaced along the Exiles Thrust system. This fault system, together with the Wilson Thrust (WT) forms a pop-up structure in the Wilson Terrane (Flöttmann et al., 1993). Our new aeromagnetic data suggest that mylonites, likely associated with the Exiles Thrust system extend along the eastern margin of the Wilkes Subglacial Basin and connect with the Priestley Fault, implying structural controls on the margin of basin. In addition our aeromagnetic imaging suggests that the Prince Albert Fault System (Ferraccioli and Bozzo, 2003) continues along the eastern margin of the Wilkes Subglacial Basin.

explained by hypothesising the existence of a broad inherited backarc basin, of Ross-age. This hypothesis is supported by the similarity in magnetic anomaly patterns over the WSB and the backarc mobile belt of the northern Cordillera (Fig. 10), and by the presence of magnetic intrusives detected within the WSB (Figs. 7 and 8), which are reminiscent of backarc intrusions—e.g. over the Antarctic Peninsula subduction system (Johnson, 1999; Ferraccioli et al., 2006). As discussed further in the following section, an alternative, but currently less favoured explanation for the width of this part of the WSB, is post-Ross, large-scale crustal extension beneath the WSB (Ferraccioli et al., 2001), overprinting the Ross-orogenic structural edifice.

9.3. Tectonic evolution of the Wilkes Subglacial Basin

The high-frequency aeromagnetic anomalies we detected in the WSB are inferred to relate to Jurassic Ferrar rocks intruding Beacon Supergroup sediments, which outcrop at Horn Bluff (Mawson, 1940), along the northern margin of the WSB (Fig. 9) Pavlov (1958) and Ravich et al. (1968) interpreted the exposed sandstones of Horn Bluff as Permian to Triassic in age from palynological evidence. Barret (1991) presented a paleogeographic model that includes thin (<500 m) Late Permian and Triassic sedimentation in the Wilkes Subglacial Basin region and further outboard in Northern Victoria

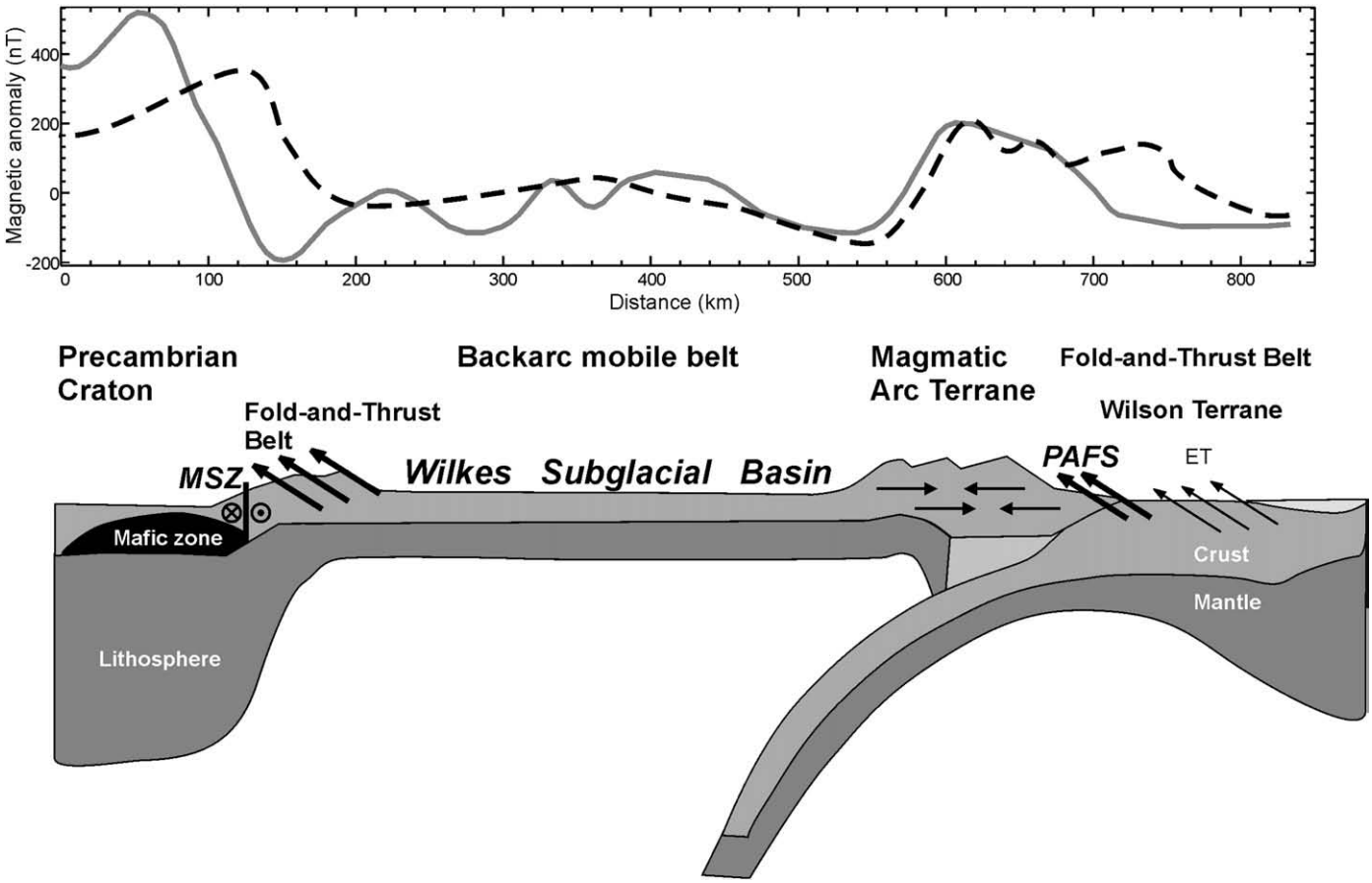

Fig. 10. The upper panel shows our aeromagnetic data (grey line) upward continued to 10 km along a profile across the Wilkes Subglacial Basin and adjacent Transantarctic Mountains (grey line in Fig. 4a). The dashed black line shows aeromagnetic data over the northwest Cordilleran margin upward continued to the same elevation, and is taken from Saltus and Hudson (2007). Note the broad similarity in magnetic anomaly pattern. Lower panel is a conceptual model for the tectonic origin of the Wilkes Subglacial Basin, based upon the analogy with magnetic signatures over the northwest Cordilleran margin. Our tectonic model suggests that the Wilkes Subglacial Basin forms the transition between the Precambrian Craton and the Ross Orogen. It contains a former backarc mobile belt, fold-and thrust belts and an accreted(?) magmatic arc terrane along its eastern flank. As in the case for the northern Cordillera, mafic rocks at the edge of the Precambrian craton may have acted a buttress for the mobile belt. The location of the Mertz Shear Zone (MSZ), Prince Albert Fault System (PAFS), and Exiles Thrust (ET) is also shown.

Land (see Figures 3.8 and 3.15 in Barret, 1991). The tectonic setting in which the Beacon sediments of the TAM and WSB were deposited is debated. Back-arc (Dalziel and Elliot, 1982), foreland basin (Collinson, 1997), intractratonic basins (Woolfe, 1989), and intermontane (Isbell, 1999) settings have been previously proposed. Oversnow gravity collected along the East-93 traverse crossing the WSB further south (Figs. 1 and 9) have been interpreted to support a possible foreland basin setting for the Beacon sediments (ten Brink et al., 1997). Analysis of more extensive aerogravity data over the northern WSB region (Jordan et al., 2007) may shed new light into the Beacon basin.

Our interpretation that high frequency magnetic anomalies in the northern WSB region are caused by Ferrar rocks intruding Beacon sediments is supported not only by regional geological considerations but also by the similarity in magnetic anomaly patterns over exposed occurrences of these rocks over the Prince Albert Mountains in the TAM (Ferraccioli and Bozzo, 1999), and over Horn Bluff and the Mawson Peninsula (Fig. 9) along the northern margin of the WSB (Damaske et al., 2003). Our interpretation is also consistent with previous magnetic interpretations along the ITASE traverse and AEROTAM survey further to the south in the WSB (Ferraccioli et al., 2001; Studinger et al., 2004). In addition, both our airborne radar data and previous ice-penetrating data identified subglacial mesa topography interpreted as being caused by Ferrar dolerites sills intruding Beacon sedimentary strata (Steed, 1983; Ferraccioli et al., 2001; Studinger et al., 2004). In some cases prominent high-frequency magnetic anomalies have been identified in areas where no mesa-topography exists, and the sources of these anomalies have been modelled both by us (Fig. 7) and previously (Fig. 5 in Studinger et al., 2004) as major dyke-like feeder bodies for Jurassic sill complexes.

The occurrence of such widespread Jurassic tholeiitic magmatism, coupled with geological evidence for Jurassic extension over the adjacent TAM (Wilson, 1993), suggests that the WSB region was, at least partially, reactivated in an extensional regime, and may perhaps have formed a Jurassic volcano-tectonic rift zone. This inference would be consistent with the occurrence of linear aeromagnetic patterns over the Prince Albert Mountains block of the TAM, which may be indicative of Jurassic rift fabric (Chiappini et al., 2002). The lack of major rift bounding faults exposed over the TAM (Elliot and Fleming, 2004) could be explained by hypothesising that the major locus of Jurassic rifting was under the WSB. The lack over the WSB of high-amplitude aeromagnetic anomalies typically associated with Cenozoic magmatism of the TAM, including both early Cenozoic intrusions and later Neogene volcanism (Rocchi et al., 2002; Smellie et al., 2007), argues against the existence of a highly magmatic Cenozoic rift zone under the WSB, comparable to the western Ross Sea Rift (Fig. 9). However, geological evidence over the western margin of the TAM suggests that the inherited Ross-age structures flanking the eastern margin of the WSB were not fossil, and may have been reactivated in the Cenozoic as major right-lateral strike–slip faults (Salvini et al., 1997). Kleinschmidt and Läufer (2006) suggested that the inherited Ross-age ductile Exiles Thrust system over Oates Land may have been reactivated in the Cenozoic to form the Matusevich Fracture Zone, a major brittle dextral

strike–slip fault zone. Dextral Cenozoic strike–slip motion has been interpreted along the Priestley Fault (Storti et al., 2001) and the occurrence of pseudotachylytes along this fault attests to seismic activity along the fault at about 34 Ma (Di Vincenzo et al., 2004). Additionally, Rossetti et al. (2006) presented seismic interpretations indicating that strike–slip faulting is likely to have continued in Neogene times, at least along the offshore trace of the Campbell and Priestley faults. In light of aeromagnetic evidence for the possible connection between the Priestley Fault located at the Ross Sea coast and the Matusevich Fracture Zone over Oates Land (Fig. 9), it appears plausible that Cenozoic reactivation of the entire eastern margin of the WSB has occurred.

Storti et al. (2007) suggested that differential transform motion in the Southern Ocean between Australia and Antarctica was accommodated by a broad region of Cenozoic intraplate right-lateral strike–slip deformation in East Antarctica. In their geodynamic model deformation occurs east of the George V transform fault (Fig. 1). If this regional geodynamic model holds true, then it may be possible to invoke Cenozoic strike–slip intraplate deformation not only over the TAM, as suggested by geological and geophysical data (Salvini et al., 1997; Ferraccioli and Bozzo, 2003; Storti et al., 2007), but also within the WSB. Over the TAM, Cenozoic strike–slip deformation along inherited fault zones is interpreted to have induced transtensional opening of localised graben structures, such as the Rennick Graben (Rossetti et al., 2003). Our magnetic model suggests the presence of localised graben-like structures in the area of the Central Basins in the WSB (Fig. 7). Graben-like features in this part of the WSB were also inferred by Masolov et al. (1981) and Kadmina et al. (1983) based upon reconnaissance radar data of Steed and Drewry (1982). We speculate, that these graben-like structures in the WSB may relate to transtensional reactivation of inherited Ross-age fault zones, as proposed by Rossetti et al. (2003) for the Rennick Graben region. Fitzgerald (2002) interpreted apatite-fission track data along the westernmost exposures of the TAM as indicating that Cretaceous to Early Cenozoic denudation may have occurred along the eastern flank of the WSB and hence that some extension may have taken place in the basin. In the Fitzgerald (2002) model a possible kinematic connection between the Rennick Graben and the WSB is also hypothesised, although a Cretaceous age for possible crustal extension is preferred.

Analysis of crustal thickness patterns beneath the WSB and the TAM could assist in testing whether the basin is, at least in part, affected by crustal extension thereby providing useful information on any possible Mesozoic and Cenozoic tectonic reactivation of the WSB region. However, estimates of crustal thickness beneath the WSB and adjacent TAM are currently few. Stern and ten Brink (1989) argued that the WSB is a glaciated flexural basin (Fig. 2b) of Cenozoic age underlain by 45 km thick crust of the East Antarctic Craton. However, gravity modelling along the ITASE traverse (Fig. 2c) imaged crust only 31 ± 2 km thick beneath the WSB, in contrast to 37 ± 3 km thick crust under the adjacent Prince Albert Mountains of the TAM (Ferraccioli et al., 2001). Models of aerogravity data along the AEROTAM corridor across the WSB (Fig. 9) also suggest relatively thinner crust beneath the basin compared to the TAM (Studinger et al., 2004). However, they attributed this pattern to crustal thickening beneath the TAM (i.e. the mountains would be underlain by a crustal root) rather than to crustal extension beneath the WSB, for which they favour a compressional tectonic origin linked to the Ross Orogen, i.e. broadly similar to our current aeromagnetic interpretation (Fig. 10). Wide-angle seismic data across the TAM are restricted to two profiles one across the Prince Albert Mountains (Della Vedova et al., 1997) and one across the transition between the Deep Freeze Range (Fig. 9) and the Ross Sea Rift (O'Connell and Stepp, 1993). Both these experiments indicate thicker crust beneath the TAM compared to the Ross Sea Rift, with maximum estimates of 37 km (Della Vedova et al., 1997), but provide no information on crustal thickness beneath the WSB. More recent seismological data further to the south indicate 40 ± 2 km crust under the TAM, and 35 ± 2 km in the hinterland of the TAM (Lawrence et al., 2006), consistent with aerogravity estimates over the central TAM (Studinger et al., 2006). Recent numerical experiments have led to suggestion that the reason why the TAM are apparently underlain by a crustal root, is that they form the edge of a collapsed plateau with thick crust, which was formerly present over the West Antarctic Rift System (Bialas et al., 2007).

Inversion of new aerogravity data collected as part of the ISODYN\WISE survey (Jordan et al., 2007) and receiver function analysis along a seismological profile crossing the WSB and adjacent TAM (Demartin and Roselli, 2007), may assist in the estimation of possible crustal thickness variations beneath the range, and under the deep subglacial basins we imaged from our new airborne radar and aeromagnetic data across the WSB.

9.4. Question of ages of possible sedimentary infill in the Wilkes Subglacial Basin

Reworked microfossil assemblages in the Sirius Formation have been interpreted to record periods of marine sedimentation in the WSB region during the Late Cretaceous, Paleocene, Eocene, late Miocene, and as late as the Pliocene (Webb et al., 1984). The possible presence of post-Jurassic sediments in the WSB inferred by Webb et al. (1984), would appear to be consistent with the interpretation of reconnaissance geophysical profiles across the basin by Drewry (1976). However, both the age of marine diatoms within the Sirius Formation and the postulated glacial transport mechanism for the marine diatoms from the WSB region proposed by Webb et al. (1984) are highly controversial (Stroeven, 1997).

Flexural gravity models for the TAM and adjacent WSB (ten Brink et al., 1997) along the East-93 traverse (Fig. 2b) have been used to argue that there is no geophysical support in favour of any sedimentary infill in the WSB, in agreement with the stabilists view of the EAIS (e.g. Sugden et al., 1995). However, our depth to magnetic source calculations and models (Figs. 6 and 7) indicate that post-Jurassic sedimentary infill in the WSB cannot be ruled out. Nevertheless, potential post-Jurassic sedimentary infill appears to be significantly more localised, and generally thinner (<1 km) in the WSB than the 400 km-wide and 3 km-deep sedimentary basin suggested by Drewry (1976). Our aeromagnetic findings are in general agreement with recent depth to magnetic source estimates based upon aeromagnetic data and aerogravity-derived estimates along the AEROTAM transect further to the south (Studinger et al., 2004). However, in our survey area the Central Basins contain localised and deeper graben-like features with a potentially thicker post-Jurassic sedimentary infill (up to a maximum of 2 km).

Our new aeromagnetic data suggests that major Cenozoic rift basins with over 5 km of sedimentary infill, such as the Victoria Land Basin in the Ross Sea Rift (Fig. 9) (Davey and Brancolini, 1995), can be regarded as unlikely beneath the WSB. Although several-km thick sedimentary basins are imaged beneath the Western Basins in the WSB (Fig. 7), our preferred interpretation is that these deeper sedimentary basins are significantly older inherited features rather than Mesozoic or Cenozoic rift basins. We propose instead the existence of thick Ross-age sedimentary infill in the Western Basins based on a recent study of a glacial erratic from the Ninnis Glacier area (Fig. 9) by Di Vincenzo et al. (2007). The glacial erratic is petrographically similar to low-grade metasedimentary xenoliths occurring in Cambro–Ordovician granites outcropping along the western side of Ninnis Glacier, which yielded detrital white-mica ^{40}Ar–^{39}Ar ages from 530 to 640 Ma, and a minimum age of 518 ± 5 Ma (Di Vincenzo et al., 2007). Whether Permian–Triassic Beacon sediments also infill the Western Basins remains uncertain. However, the Western Basins clearly lie west of Horn Bluff, the westernmost outcrop of these rocks (Fig. 9). In addition, high-frequency magnetic anomalies related to Jurassic sills, which typically intrude Beacon

sediments, are lacking over the Western Basins (Fig. 3b). It may also be conceivable that more recent reactivation of the Western Basins has occurred, forming localised Mesozoic to Cenozoic upper-crustal grabens super-imposed upon the older sedimentary basins. In this scenario the lack of high frequency aeromagnetic anomalies could be explained by assuming the occurrence of post-Jurassic sedimentary infill, as we proposed for the Central Basins. Notably, the presence of rift-related grabens in the area of the Western Basins was inferred by Masolov et al. (1981) and Kadmina et al. (1983), based on the regional sub-ice morphology (Steed and Drewry, 1982) and continental-scale depth to magnetic basement estimates. However, no aeromagnetic data were available over this sector of the WSB to construct the map, and hence the continental-scale interpretations should be looked upon with caution. In addition, there is no independent geological evidence for any reactivation of the Precambrian Mertz Shear Zone, forming the western flank of the Western Basins, or any record from glacial erratics found in the Ninnis Glacier area of post-Ross-age sedimentary rocks. Drilling offshore the WSB is planned as part of IODP and may provide new data on the ages of the inferred sedimentary infill in this region (C. Escutia pers. comm., 2008).

10. Conclusions

Aeromagnetic anomaly data, coupled with airborne radar imaging over the EAIS, have provided a new view of the enigmatic WSB, in the hinterland of the TAM. Our airborne radar data reveals that this part of the WSB contains several deep basins we named the Eastern Basins, the Central Basins and the Western Basins, which are separated by major subglacial highlands. Aeromagnetic data have been used to investigate the subglacial geology and tectonic origin of the WSB and its newly imaged sub-basins. Prominent aeromagnetic lineaments on both flanks of the WSB suggest that the basin is structurally controlled, rather than a simple flexural downwarp (Stern and ten Brink, 1989), induced by Cenozoic uplift of the TAM. The eastern margin of the WSB was imposed upon a major Ross-age thrust fault belt, which was reactivated as a right-lateral strike–slip intraplate deformation zone, in the Cenozoic. The western margin of the WSB is imposed upon a major fold-and-thrust belt of Ross-age, in the area of the Western Basins. Further to the west it is flanked, by the inferred continuation of the Mertz Shear Zone, a major Precambrian strike–slip fault (Talarico and Kleinschmidt, 2003; Di Vincenzo et al., 2007).

Comparison between aeromagnetic patterns over the WSB and the northern Cordillera in Canada and Alaska (Saltus and Hudson, 2007), suggests that the WSB is imposed upon a broad transition zone between a magmatic arc, of Ross-age, and the Precambrian East Antarctic Craton, and contains a major backarc basin and craton-ward fold-and-thrust belts. The mafic rocks we imaged at the leading edge of the Precambrian craton likely acted as a back-stop for Ross-age deformation.

High-frequency aeromagnetic anomalies over the WSB reveal the subglacial extent of Jurassic rocks of the Ferrar Group, intruded into Beacon sediments that outcrop along the northern margin of the basin at Horn Bluff. We interpret these Jurassic tholeiites as having being emplaced in a possible volcano-tectonic rift zone within the WSB. The lack of high-amplitude aeromagnetic anomalies, typically associated with Cenozoic rift-related magmatism over the TAM and adjacent Ross Sea Rift, suggests that any possible later Cenozoic extension in the WSB was largely amagmatic. In addition, Cenozoic rift basins with thick sedimentary infill across the width of the WSB appear unlikely from our aeromagnetic analysis. However, more localised upper crustal graben-like features with sedimentary infill are inferred to exist beneath the newly imaged Central Basins. These graben-like structures may speculatively relate to transtensional reactivation of faults in the WSB, perhaps induced by regional Cenozoic intraplate strike–slip faulting (Storti et al., 2007). Alternatively or additionally they may relate to regional Cretaceous extension (Fitzgerald, 2002).

Acknowledgements

This paper is a contribution to the joint UK-Italian ISODYN (Icehouse Earth: Stability or Dynamism?) and WISE (Wilkes Basin/Transantarctic Mountains System Exploration) projects. We gratefully acknowledge the suggestions made by three anonymous reviewers that greatly improved the manuscript. We wish to thank all our engineering staff for their support and assistance in the field, including Carl Robinson and Nick Frearson (BAS), and Giorgio Caneva from DIPTERIS, Univ. di Genova. Logistic support and aviation fuel during the joint campaign was provided by PNRA, with BAS providing the aerogeophysical platform. We would like to thank Giuseppe De Rossi and Alberto Della Rovere, and their PNRA teams, for making all the complex logistics for the campaign available to us. All the staff at the Mario Zucchelli Station, are gratefully thanked both for their hospitality and for their support. Mike Dinn (BAS) is gratefully thanked, for his assistance, when planning and negotiating all the logistic deployments. Very special thanks go to the BAS Air-unit, in particular to our pilot, David Leatherdale, who did a truly outstanding job. Our BAS aircraft engineer Kyle Hegadus (Fields Aviation) is also acknowledged for his aircraft maintenance work. Thanks also go to all the team involved in the independent TALDICE deep ice-drilling project, which was sharing the remote field camp with us at Talos Dome.

References

Adams, C.J., 2006. Style of uplift of Paleozoic Terranes in Northern Victoria Land, Antarctica: evidence from K–Ar age patterns. In: Futterer, D.K., Damaske, D., Kleinschmidt, G., Miller, H., Tessensohn, F. (Eds.), Antarctica—Contributions To Global Earth Sciences. Springer, pp. 205–214.

Armadillo, E., Ferraccioli, F., Tabellario, G., Bozzo, E., 2004. Electrical structure across a major ice-covered fault belt in Northern Victoria Land (East Antarctica). Geophysical Research Letters 31, 10615. doi:10.1029/2004GL019903.

Barret, P.J., 1991. The Devonian to Jurassic Beacon Supergroup of the Transantarctic Mountains and correlatives in other parts of Antarctica. In: Tingey, R.J. (Ed.), The Geology of Antarctica. Oxford Monographson Geology and Geophysics, vol. 17, pp. 120–152.

Behrendt, J.C., Saltus, R., Damaske, D., McCafferty, A., Finn, C.A., Blankenship, D., Bell, R.E., 1996. Patterns of late Cenozoic volcanic and tectonic activity in the West Antarctic Rift System revealed by aeromagnetic surveys. Tectonics 15, 660–676.

Behrendt, J.C., Blankenship, D.D., Morse, D.L., Bell, R.E., 2004. Shallow-source aeromagnetic anomalies observed over the West Antarctic Ice Sheet compared with coincident bed topography from radar ice sounding—new evidence for glacial "removal" of subglacially erupted late Cenozoic rift-related volcanic edifices. Global and Planetary Change 42 (1–4), 177–193.

Bell, R., Blankenship, D.D., Finn, C.A., Morse, D.L., Scambos, T.A., Brozena, J.M., Hodge, S.M., 1998. Influence of subglacial geology on the onset of a West Antarctic ice stream from aerogeophysical observations. Nature 394, 58–62.

Bell, R.E., Studinger, M., Karner, G.D., Finn, C.A., Blankenship, D.D., 2006. Identifying major sedimentary basins beneath the West Antarctic Ice Sheet from aeromagnetic data analysis. In: Fütterer, D.K., Damaske, D., Kleinschmidt, G., Miller, H., Tessensohn, F. (Eds.), Antarctica: Contributions to Global Earth Sciences. Springer-Verlag, Berlin, pp. 117–122.

Bialas, R.W., Buck, W.R., Studinger, M., Fitzgerald, P.G., 2007. Plateau collapse model for the Transantarctic Mountains–West Antarctic Rift System: insights from numerical experiments. Geology 35, 687–690. doi:10.1130/G23825A.1.

Blakely, R.J., 1995. Potential Theory in Gravity and Magnetic Applications. Cambridge University Press. 441 pp.

Blakely, R.J., Simpson, R.W., 1986. Approximating edges of source bodies from magnetic or gravity anomalies. Geophysics 51, 1494–1498.

Blankenship, D.D., Bell, R.E., Hodge, S.M., Brozena, J.M., Behrendt, J.C., Finn, C.A., 1993. Active volcanism beneath the West Antarctic ice sheet and implications for ice-sheet stability. Nature 361, 526–529.

Blankenship, D.D., Morse, D.L., Finn, C.A., Bell, R.E., Peters, M.E., Kempf, S.D., Hodge, S.M., Studinger, M., Behrendt, J.C., Brozena, J.M., 2001. Geologic controls on the initiation of rapid basal motion for West Antarctic ice streams: a geophysical perspective including new airborne radar sounding and laser altimetry results. In: Alley, R.B., Binschadler, R.A. (Eds.), The West Antarctic Ice Sheet: Behavior and Environment. Antarct. Res. Ser., vol. 77. AGU, Washington, D. C., pp. 105–121.

Bosum, W., Damaske, D., Roland, N.W., Behrendt, J.C., Saltus, R., 1989. The GANOVEX IV Victoria Land/Ross Sea aeromagnetic survey: interpretation of the anomalies. Geologisches Jahrbuch E38, 153–230.

Bozzo, E., Colla, A., Meloni, A., 1992. Ground magnetics in North Victoria Land (East Antarctica). In: Yoshida, Y., Kaminuma, K., Shiraishi, K. (Eds.), Recent Progress in Antarctic Earth Science. Terra Scientific Publishing Company, Tokyo, pp. 563–569.

Bozzo, E., Caneva, G., Capponi, G., Colla, A., 1995. Magnetic investigations of the junction between Wilson and Bowers Terranes (northern Victoria Land, Antarctica). Antarct. Sci. 7 (2), 149–157.

Cande, S.C., Stock, J.M., Müller, R.D., Ishihara, T., 2000. Cenozoic motion between East and West Antarctica. Nature 404, 145–150.

Cape Roberts Science Team, 2000. Summary of results. In: Barrett, P.J., Sarti, M., Sherwood, W. (Eds.), Initial Report on CRP-3. Terra Antartica. Siena, pp. 185–209.
Chiappini, M., Ferraccioli, F., Bozzo, E., Damaske, D., 2002. Regional compilation and analysis of aeromagnetic anomalies for the Transantarctic Mountains–Ross Sea sector of the Antarctic. Tectonophysics 347 (1–3), 121–137.
Collinson, J.W., 1997. Paleoclimate of Permo-Triassic Antarctica. In: Ricci, C.A. (Ed.), The Antarctic Region: Geological Evolution and Processes. Terra Antartica. Siena, pp. 1029–1034.
Cooper, G.R.J., Cowan, D.R., 2006. Enhancing potential field data using filters based on the local phase. Computers & Geosciences 32 (10), 1585–1591.
Cooper, A.K., Davey, F.J., Behrendt, J.C., 1987. Seismic stratigraphy and structure of the Victoria Land Basin, western Ross Sea, Antarctica. In: Cooper, A.K., Davey, F.J. (Eds.), The Antarctic Continental Margin Geology and Geophysics of the Western Ross. SeaEarth Sci. Ser., vol. 5B. Circum-Pacific Council for Energy and Natural Resources, Houston, pp. 27–76.
Cordell, L.E., Grauch, V.J.S., 1985. Mapping basement magnetization zones from aeromagnetic data in the San Juan Basin, New Mexico. In: Hinze, W.J. (Ed.), The utility of regional gravity and magnetic anomaly maps. Soc. Explor. Geophys., pp. 181–197.
Corr, H., Ferraccioli, F., Frearson, N., Jordan, T., Robinson, C., Armadillo, E., Caneva, G., Bozzo, E., Tabacco, I., 2007. Airborne radio-echo sounding of the Wilkes Subglacial Basin, the Transantarctic Mountains, and the Dome C region. In: Bozzo, E., Ferraccioli, F. (Eds.), The Italian–British Antarctic Geophysical and Geological Survey in Northern Victoria Land 2005–06—towards the International Polar Year 2007–08. Terra Antartica Reports, vol. 13, pp. 55–63.
Dalziel, I.W.D., Elliot, D.H., 1982. West Antarctica: problem child of Gondwanaland. Tectonics 1, 3–19.
Damaske, D., 1994. Aeromagnetic surveys over the Transantarctic Mountains and the Ross Sea area. Terra Antartica 1 (3), 503–506.
Damaske, D., Ferraccioli, F., Bozzo, E., 2003. Aeromagnetic anomaly investigation along the Antarctic coast between Yule Bay and Mertz Glacier. Terra Antartica 10 (3), 197–220.
Davey, F.J., Brancolini, G., 1995. The Late Mesozoic and Cenozoic structural setting of the Ross Sea Region. In: Cooper, A.K., Brancolini, G. (Eds.), Geology and seismic stratigraphy of the Antarctic Margin. AGU Ant. Res. Ser, vol. 68, pp. 167–182.
Davey, F.J., De Santis, L., 2006. A multi-phase rifting model for the Victoria Land Basin, Western Ross Sea. In: Fütterer, D.K., Damaske, D., Kleinschmidt, G., Miller, H., Tessensohn, F. (Eds.), Antarctica: Contributions to Global Earth Sciences, Springer-Verlag, Berlin Heidelberg New York, pp. 117–122, 303–308.
Decesari, R.C., Wilson, D.S., Luyendyk, B.P., Faulkner, M., 2007. Cretaceous and Tertiary extension throughout the Ross Sea, Antarctica. In: Cooper, A., Raymond, C. (Eds.), Antarctica: A Keystone in a Changing World—Online Proceedings of the 10th ISAES. Vol. Short Research Paper 098. USGS Open-File Report. doi:10.3133/of2007-1047.srp098.
Della Vedova, B., Pellis, G., Trey, H., Zhang, J., Cooper, A.K., Makris, J., ACRUP Working Group, 1997. Crustal structure of the Transantarctic Mountains, Western Ross Sea. In: Ricci, C.A. (Ed.), The Antarctic Region: Geological Evolution and Processes. Terra Antartica Pub., pp. 609–618.
Demartin, M., Roselli, P., 2007. Seismological experiment across the Wilkes Subglacial Basin and adjacent Transantarctic Mountains. In: Bozzo, E., Ferraccioli, F. (Eds.), The Italian–British Antarctic Geophysical and Geological Survey in Northern Victoria Land 2005–06-towards the International Polar Year 2007–08. Terra Antartica Reports, vol. 13, pp. 75–86.
Di Vincenzo, G., Rocchi, S., Rossetti, F., Storti, F., 2004. Ar—Ar dating of pseudotachylytes: the effect of clast-hosted extraneous argon in Cenozoic fault-generated friction melts from the West Antarctic Rift System. Earth and Planet. Sci. Lett. 223, 349–364.
Di Vincenzo, G., Talarico, F., Kleinschmidt, G., 2007. An ^{40}Ar–^{39}Ar investigation of the Mertz Glacier area (George V Land, Antarctica): implications for the Ross Orogen–East Antarctic Craton relationship and Gondwana reconstructions. Precambrian Research 152, 93–118. doi:10.1016/j.precamres.2006.10.002.
Drewry, D.J., 1976. Sedimentary basins of the East Antarctic Craton from geophysical evidence. Tectonophysics 36, 301–314.
Drewry, D.J., 1983. Antarctica: Glaciological and Geophysical Folio. Scott Polar Res. Inst., University Cambridge, Cambridge. 9 sheets.
Elliot, D.H., Fleming, T.H., 2004. Occurrence and dispersal of magmas in the Jurassic Ferrar Large Igneous Province, Antarctica. Gondwana Research 7, 223–236. doi:10.1016/S1342-937X(05)70322-1.
Encarnacion, B.J., Fleming, T.H., Elliot, D.H., Eales, H.V., 1996. Synchronous emplacement of Ferrar and Karoo dolerites and the early breakup of Gondwana. Geology 24, 535–538.
Fanning, C.M., Ménot, R.P., Pecaut, J.J., Pelletier, A., 2002. A closer examination of the direct links between southern Australia and Terre Adélie and George V Land. In: Preiss, V.P. (Ed.), Geosciences 2002: Expanding Horizons. Abstracts of the 16th Australian Geological Conference, vol. 67 Adelaide, p. 224.
Federico, L., Capponi, G., Crispini, L., 2006. The Ross Orogeny of the Transantarctic Mountains: a northern Victoria Land perspective. Int. J. Earth. Sci 95 (5), 759–770.
Ferraccioli, F., Bozzo, E., 1999. Inherited crustal features and tectonic blocks of the Transantarctic Mountains: an aeromagnetic perspective (Victoria Land, Antarctica). J. Geophys. Res. 104, 25297–25320.
Ferraccioli, F., Bozzo, E., 2003. Cenozoic strike–slip faulting from the eastern margin of the Wilkes Subglacial Basin to the western margin of the Ross Sea Rift: an aeromagnetic connection. In: Storti, F., Holdsworth, R.E., Salvini, F. (Eds.), Intraplate Strike–slip Deformation. J. Geol. Soc. Spec. Publ., vol. 210, pp. 109–133.
Ferraccioli, F., Gambetta, M., Bozzo, E., 1998. Microlevelling procedures applied to regional aeromagnetic data: an example from the Transantarctic Mountains (Antarctica). Geophysical Prospecting 46 (2), 177–196.
Ferraccioli, F., Coren, F., Bozzo, E., Zanolla, C., Gandolfi, S., Tabacco, I., Frezzotti, M., 2001. Rifted(?) crust at the East Antarctic Craton margin: gravity and magnetic interpretation along a traverse across the Wilkes Subglacial Basin region. Earth and Planet. Sci. Lett. 192, 407–421.
Ferraccioli, F., Bozzo, E., Capponi, G., 2002. Aeromagnetic and gravity anomaly constraints for an early Paleozoic subduction system of Victoria Land, Antarctica. Geophys. Res. Lett. 29, 10. doi:10.1029/2001GL014138.
Ferraccioli, F., Damaske, D., Bozzo, E., Talarico, F., 2003. The Matusevich aeromagnetic anomaly over Oates Land, East Antarctica. Terra Antartica 10 (3), 221–228.
Ferraccioli, F., Jones, P.C., Vaughan, A.P.M., Leat, P.T., 2006. New aerogeophysical view of the Antarctic Peninsula: more pieces, less puzzle. Geophysical Research Letters 33, L05310. doi:10.1029/2005GL024636.
Ferraccioli, F., Jordan, T., Armadillo, E., Bozzo, E., Corr, H., Caneva, G., Robinson, C., Frearson, N., Tabacco, I., 2007. Collaborative aerogeophysical campaign targets the Wilkes Subglacial Basin, the Transantarctic Mountains and the Dome C region. In: Bozzo, E., Ferraccioli, F. (Eds.), The Italian–British Antarctic Geophysical and Geological Survey in Northern Victoria Land 2005–06—Towards the International Polar Year 2007–08. Terra Antartica Reports, vol. 13, pp. 1–36.
Finn, C.A., 1994. Aeromagnetic evidence for a buried early Cretaceous magmatic arc, northeast Japan. J. Geophys. Res. 99, 22,165–22,185.
Finn, C.A., Moore, D., Damaske, D., Mackey, T., 1999. Aeromagnetic legacy of early Paleozoic subduction along the Pacific margin of Gondwana. Geology 27 (12), 1087–1090.
Finn, C.A., Goodge, J.W., Damaske, D., Fanning, C.M., 2006. Scouting craton's edge in paleo-Pacific Gondwana. In: Fütterer, D.K., Damaske, D., Kleinschmidt, G., Miller, H., Tessensohn, F. (Eds.), Antarctica: Contributions to Global Earth Sciences. Springer-Verlag, Berlin, pp. 165–174.
Fitzgerald, P., 2002. Tectonics and landscape evolution of the Antarctic plate since the breakup of Gondwana, with an emphasis on the West Antarctic Rift System and the Transantarctic Mountains. In: Gamble, J.A., Skinner, D.N.B., Henrys, S. (Eds.), Antarctica at the close of a millenium. Proceedings of the 8th International Symposium on Antarctic Earth Sciences. Royal Society of New Zealand Bulletin, vol. 35. SIR publishing, pp. 453–469.
Flöttmann, T., Kleinshmidt, G., 1991. Opposite thrust systems in northern Victoria Land, Antarctica: imprints of Gondwana's Paleozoic accretion. Geology 19, 45–47.
Flöttmann, T., Gibson, G.M., Kleinschmidt, G., 1993. Structural continuity of the Ross and Delamerian orogens of Antarctica and Australia along the margin of the paleo-Pacific. Geology 21, 319–322.
Flöttmann, T., James, P., Rogers, J., Johnson, T., 1994. Early Paleozoic foreland thrusting and basin reactivation at the Paleo-Pacific margin of the southeastern Australian Precambrian craton: a reappraisal of the structural evolution of the Southern Adelaide Fold–Thrust Belt. Tectonophysics 23, 95–116.
GANOVEX Team, 1987. Geological map of North Victoria Land, Antarctica: explanatory notes. Geologisches Jahrbuch B66, 7–79.
Hamilton, R.J., Luyendyk, B.P., Sorlein, C.C., Bartek, L.R., 2001. Cenozoic tectonics of the Cape Roberts rift basin and Transantarctic Mountains front, southwestern Ross Sea, Antarctica. Tectonics 20, 325–342.
Huerta, A.D., Harry, D.L., 2007. The transition from diffuse to focused extension: modelled evolution of the West Antarctic Rift system. Earth and Planetary Science Letters 255, 133–147.
Isbell, J.L., 1999. The Kukri erosional surface: a reassessment of its relationship to rocks of the Beacon Supergroup in the central Transantarctic Mountains, Antarctica. Antarctic Science 11, 222–238.
Johnson, A.C., 1999. Interpretation of new aeromagnetic anomaly data from the central Antarctic Peninsula. J. Geophys. Res. 104, 5031–5046.
Jordan, T., Ferraccioli, F., Corr, H., Robinson, C., Caneva, G., Armadillo, E., Bozzo, E., Frearson, N., 2007. Linking the Wilkes Subglacial Basin, the Transantarctic Mountains, and the Ross Sea with a new airborne gravity survey. In: Bozzo, E., Ferraccioli, F. (Eds.), The Italian–British Antarctic Geophysical and Geological Survey in Northern Victoria Land 2005–06—towards the International Polar Year 2007–08. Terra Antartica Reports, vol. 13, pp. 37–54.
Kadmina, I.N., Kurinin, R.G., Masolov, V.N., Grikurov, G.E., 1983. Antarctic crustal structure from geophysical evidence a review. In: Oliver, R.L., James, P.R., Jago, J.B. (Eds.), Antarctic Earth Science. Australian Academy of Science, Canberra, pp. 498–502.
Karner, G.D., Studinger, M., Bell, R.E., 2005. Gravity anomalies of sedimentary basins and their mechanical implications: application to the Ross Sea basins, West Antarctica. Earth and Planetary Science Letters 235, 577–596.
Kleinschmidt, G., Läufer, A.L., 2006. The Matusevich fracture zone in Oates Land, East Antarctica. In: Fütterer, D.K. (Ed.), Antarctica: Contributions to global earth sciences. Springer, Heidelberg, pp. 175–180.
Ku, C.C., Sharp, J.A., 1983. Werner deconvolution for automated magnetic interpretation and its refinement using Marquardt inverse modeling. Geophysics 48 (6), 754–774.
Läufer, A.L., Kleinschmidt, G., Rossetti, F., 2006. Late-Ross structures in the Wilson Terrane in the Rennick Glacier area (Northern Victoria Land, Antarctica). In: Fütterer, D.K., Damaske, D., Kleinshmidt, G., Miller, H., Tessensohn, F. (Eds.), Antarctica—Contributions to Global Earth Sciences. Springer, Heidelberg, pp. 195–200.
Lawrence, J.F., Wiens, D.A., Nyblade, A.A., Anandakrishnan, S., Shore, P.J., Voigt, D., 2006. Crust and upper mantle structure of the Transantarctic Mountains and surrounding regions from receiver functions, surface waves and gravity: implications for uplift models. Geochemistry, Geophysics, Geosystems 7. doi:10.1029/2006GC001282.
Lawver, L., Gahagan, L., 1994. Constraints on timing of extension in the Ross Sea Region. Terra Antartica 1, 545–552.
Lythe, M.B., Vaughan, D.G., BEDMAP Consortium, 2001. BEDMAP, a new ice thickness and subglacial topographic model of Antarctica. J. Geophys. Res. 106, 11335–11351.
Masolov, V.N., Kurinin, R.G., Grikurov, G.E., 1981. Crustal structure and tectonic significance of Antarctica rift zones (from geophysical evidence). In: Cresswell,

M.M., Vella, P. (Eds.), Gondwana V—Proceedings of the fifth International Gondwana Symposium. Wellington, New Zealand, pp. 303–309.
Maus, S., Rother, M., Holme, R., Luhr, H., Olsen, N., Haak, V., 2002. First scalar magnetic anomaly map from CHAMP satellite data indicates weak lithospheric field. Geophys. Res. Lett. 29 (14), 1702. doi:10.1029/2001GL013685.
Mawson, D., 1940. Sedimentary rocks. Australasian Antarctic Expedition 1911–1914. Scientific Reports, Series A, vol. IV(II), pp. 347–367.
O'Connell, D.H., Stepp, T.M., 1993. Structure and evolution of the crust at the Transantarctic Mountains—Ross sea crustal transition: results from the Tourmaline Plateau seismic array of the GANOVEX V ship-to-shore seismic refraction experiment. Geol. Jahrb. E47, 229–276.
Oliver, R.L., Fanning, C.M., 1997. Australia and Antarctica: precise correlation of Palaeoproterozoic terrains. In: Ricci, C.A. (Ed.), The Antarctic Region: Geological Evolution and Processes. Terra Antartica. Siena, pp. 163–172.
Pavlov, V.V., 1958. Results of palynological analysis of samples from the sedimentary-volcanic Beacon Series (Antarctica, King George V Coast, Horn Bluff). Nauk-Issl Institute of Geology Arktiki. Sbornik Stratigraphy, Palaeontology and Biostratigraphy, 12, 77, 9.
Pilkington, M., Thurston, B.J., 2001. Draping corrections for aeromagnetic data: line- versus grid-based approaches. Exploration Geophysics 32, 95–101.
Ravich, M.G., Klimov, L.V., Soloviev, D.S., 1968. The Pre-Cambian of East Antarctica. Israel Program for Scientific Translations, Jerusalem.
Reed, J.C., Wheeler, J.O., Tucholke, B.E., 2005. Geologic map of North America. Geol. Soc. of America Continental-Scale Map CSM001, scale 1:5,000,000.
Reid, A.B., Allsop, J.M., Granser, H., Millet, A.J., Somerton, I.W., 1990. Magnetic interpretation in three dimensions using Euler deconvolution. Geophysics 55 (1), 80–91.
Ricci, C.A., Talarico, F., Palmeri, R., 1997. Tectonothermal evolution of the Antarctic Paleo-Pacific active margin of Gondwana: a northern Victoria Land perspective. In: Ricci, C. (Ed.), The Antarctic Region: Geological Evolution and Processes. Terra Antartica Publ., Siena, pp. 591–596.
Rocchi, S., Tonarini, S., Armienti, P., Innocenti, F., Manetti, P., 1998. Geochemical and isotopic structure of the early Palaeozoic active margin of Gondwana in northern Victoria Land, Antarctica. Tectonophysics 284, 261–281.
Rocchi, S., Armienti, P., D'Orazio, M., Tonarini, S., Wijbrans, J.R., Di Vincenzo, G., 2002. Cenozoic magmatism in the western Ross Embayment: role of mantle plume versus plate dynamics in the development of the West Antarctic Rift System. Journal of Geophysical Research 107. doi:10.1029/2001JB000515.
Rossetti, F., Lisker, F., Storti, F., Läufer, A.L., 2003. Tectonic and denudational history of the Rennick Graben (North Victoria Land): implications for the evolution of rifting between East and West Antarctica. Tectonics 22 (2). doi:10.1029/2002TC001416.
Rossetti, F., Storti, F., Busetti, M., Lisker, F., Di Vincenzo, G., Läufer, A., Rocchi, S., Salvini, F., 2006. Eocene initiation of Ross Sea dextral faulting and implications for East Antarctic neotectonics. Journal of the Geological Society of London 163, 119–126.
Saltus, R.W., Hudson, T.L., 2007. Regional magnetic anomalies, crustal strength, and the location of the northern Cordilleran fold-and-thrust belt. Geology 35 (6), 567–570. doi:10.1130/G23470A.1.
Salvini, F., Brancolini, G., Busetti, M., Storti, F., Mazzarini, F., Coren, F., 1997. Cenozoic geodynamics of the Ross Sea region, Antarctica: crustal extension, intraplate strike–slip faulting, and tectonic inheritance. J. Geophys. Res. 102, 24669–24696.
Schmidt, D.J., Rowley, P.D., 1986. Continental rifting and transform faulting along the Jurassic Transantarctic rift, Antarctica. Tectonics 5, 279–291.
Skinner, D.N.B., 1991. Metamorphic basement contact relations, in the southern Wilson Terrane, Terra Nova Bay, Antarctica—the Boomerang Thrust. Mem. Soc. Geol. Ital 46, 163–168.
Smellie, J.L., Rocchi, S., Armienti, P., 2007. Joint Italian–British petrological–palaeoenvironmental investigations of Neogene volcanic sequences in northern Victoria Land, 2005–06. In: Bozzo, E., Ferraccioli, F. (Eds.), The Italian–British Antarctic Geophysical and Geological Survey in Northern Victoria Land 2005–06—towards the International Polar Year 2007–08. Terra Antartica Reports, vol. 13, pp. 103–110.
Steed, 1983. Structural interpretation of Wilkes Land, Antarctica. In: Oliver, R.L., James, P.R., Jago, J.B. (Eds.), Antarctic Earth Science-Proc. Fourth Int. Symp. Antarct. Earth Sci. Cambridge University Press, New York, pp. 567–572.
Steed, R.H.C., Drewry, D.J., 1982. Radio Echo Sounding Investigations of Wilkes Land, Antarctica. Univ. of Wisconsin Press, Madison, pp. 969–975.
Stern, T.A., ten Brink, U.S., 1989. Flexural uplift of the Transantarctic Mountains. Jour. Geophys. Res. 94, 10,315–10,330.
Stern, T.A., Baxter, A.K., Barrett, P.J., 2005. Isostatic rebound due to glacial incision within the Transantarctic Mountains. Geology 33, 221–224. doi:10.1130/G21068.1.
Storti, F., Rossetti, F., Salvini, F., 2001. Structural architecture and displacement accommodation mechanisms at the termination of the Priestley Fault, northern Victoria Land, Antarctica. Tectonophysics 341 (1–4), 141–161.
Storti, F., Salvini, F., Rossetti, F., Morgan, J.P., 2007. Intraplate termination of transform faulting within the Antarctic continent. Earth and Planetary Science Letters 260 (1–2), 115–126.
Stroeven, A.P., 1997. The Sirius Group of Antartica: age and environments. In: Ricci, C.A. (Ed.), The Antarctic Region: Geological Evolution and Processes. Terra Antarctica. Siena, pp. 747–761.
Studinger, M., Bell, R.E., Blankenship, D.D., Finn, C.A., Arko, R.A., Morse, D.L., Joughin, I., 2001. Subglacial sediments: a regional geological template for ice flow in West Antarctica. Geophys. Res. Lett. 28 (18), 3493–3496.
Studinger, M., Bell, R.E., Buck, W.R., Karner, G.D., Blankenship, D.D., 2004. Sub-ice geology inland of the Transantarctic Mountains in light of new aerogeophysical data. Earth Planet. Sci. Lett. 220, 391–408. doi:10.1016/S0012-821X(04)00066-4.
Studinger, M., Bell, R.E., Fitzgerald, P.G., Buck, W.R., 2006. Crustal architecture of the Transantarctic Mountains between the Scott and Reedy Glacier region and South Pole from aerogeophysical data. Earth and Planetary Science Letters 250, 189–199. doi:10.1016/j.epsl.2006.07.35.
Sugden, D.E., Denton, G.H., Marchant, D.R., 1995. Landscape evolution of the Dry Valleys, Transantarctic Mountains: tectonic implications. Journal of Geophysical Research 100, 9949–9967.
Tabacco, I.E., Cianfarra, P., Forieri, A., Salvini, F., Zirizotti, A., 2006. Physiography and tectonic setting of the subglacial lake district between Vostok and Belgica subglacial highlands (Antarctica). Geophys. J. Int. 165, 1029–1040.
Talarico, F., Kleinschmidt, G., 2003. Structural and metamorphic evolution of the Mertz Shear Zone (East Antarctic Craton, GeorgeV Land): implications for Australia/Antarctica Correlations and East Antarctic Craton/Ross Orogen relationships. Terra Antartica 10, 229–248.
Talarico, F., Armadillo, E., Bozzo, E., 2001. Antarctic rock magnetic properties: new susceptibility measurements in Oates Land and George V Land. Terra Antartica Reports 5, 45–50.
Talarico, F., Armadillo, E., Ferraccioli, F., Rastelli, N., 2003. Magnetic petrology of the Ross Orogen in Oates Land (Antarctica). Terra Antartica 10 (3), 197–220.
Talarico, F., Armadillo, E., Bozzo, E., 2007. Antarctic rock magnetic properties: new susceptibility measurements in the Daniels Range, Outback Nunataks and in the Rennick Glacier area. In: Bozzo, E., Ferraccioli, F. (Eds.), The Italian–British Antarctic Geophysical and Geological Survey in Northern Victoria Land 2005–06—towards the International Polar Year 2007–08. Terra Antartica Reports, vol. 13, pp. 87–96.
ten Brink, U., Stern, T., 1992. Rift flank uplifts and hinterland basins: comparison of the Transantarctic Mountains with the Great Escarpment of Southern Africa. J. Geophys. Res. 97, 569–585.
ten Brink, U.S., Hackney, R.I., Bannister, S., Stern, T.A., Makovsky, Y., 1997. Uplift of the Transantarctic Mountains and the bedrock beneath the East Antarctic ice sheet. J. Geophys. Res. 102, 27603–27622.
Tonarini, S., Rocchi, S., Armienti, P., 1997. Constraints on timing of Ross Sea rifting inferred from Cainozoic intrusions from northern Victoria Land, Antarctica. In: Ricci, C.A. (Ed.), The Antarctic Region: Geological Evolution and Processes, pp. 511–521.
Trey, H., Cooper, A.K., Pellis, G., Della Vedova, B., Cochrane, G., Brancolini, G., Makris, J., 1999. Transect across the West Antarctic rift system in the Ross Sea, Antarctica. Tectonophysics 301 (1–2), 61–74.
Van der Wateren, F.M., Cloetingh, S.A.P.L., 1999. Feedbacks of lithosphere dynamics and environmental change of the Cenozoic West Antarctic Rift System. Global and Planetary Change 23 (1–4), 1–24.
Webb, P.N., Harwood, D.M., McKelvey, B.C., Mercer, J.H., Scott, L.D., 1984. Cenozoic marine sedimentation and ice volume variation on the East Antarctic craton. Geology 287–291.
Wilson, T.J., 1993. Jurassic faulting and magmatism in the Transantarctic Mountains: implications for Gondwana breakup. In: Findlay, R.H., Banks, M.R., Unrug, R., Veevers, J., Balkema, A.A. (Eds.), Gondwana 8—Assembly, Evolution, and Dispersal. A.A. Balkema, Rotterdam, pp. 563–572.
Wilson, T.J., 1995. Cenozoic transtension along the Transantarctic Mountains–West Antarctic Rift boundary, southern Victoria Land, Antarctica. Tectonics 14, 531–545.
Woolfe, K.J., 1989. Tectonic setting of the Beacon Supergroup. Geological Society of New Zealand Miscellaneous Publication, 43, 108.
Woolfe, K.J., Barrett, P.J., 1995. Constraining the Devonian to Triassic tectonic evolution of the Ross Sea sector. Terra Antartica 2, 7–21.